6

Advanced Radio Interface Techniques and Performance

H. Rohling, Technical University of Braunschweig, Germany

This chapter summarises the results of the technical activities performed mainly by the Working Group 1 (WG 1) members of COST 231. WG 1 focused on general radio system aspects but in this chapter the desription of transmission techniques and their performance is given priority. A large number of technical documents and reports were written in recent years by the WG 1 members giving detailed information and analysis of radio interface techniques for 3rd generation mobile radio systems. These reports which are available in the open literature are referenced in this chapter. The different technical subjects in which WG 1 members were involved are covered in separate subsections and the names of all authors responsible for each subsection are given at the beginning of that subsection. Readers are invited to contact individual authors.

Chapter 6 is organized as follows: The first subsection deals with linear (QAM, PSK) and nonlinear (MSK, GMSK, QMSK, MAQMSK, multi-h CPM) modulation techniques which are analysed and optimised for various radio propagation conditions. Furtheron, transmitter linearisation methods are discussed in conjunction with linear modulation techniques.

Subsection 2 deals with advanced equalisation techniques and equalisation in combination with diversity. In addition, the convergence properties of the classical algorithms to perform adaptive equalisation are desribed.

Subsection 3 discusses the capacity of a cellular TDMA system which can be greatly increased if enhanced techniques such as adaptive modulation, adaptive coding or dynamic channel allocation are applied. The performance of such an enhanced TDMA system is compared with different CDMA systems in terms of spectral efficiency and capacity.

The fourth subsection in this chapter deals with CDMA which was extensively studied in WG 1. Results relating to the performance of DS-CDMA, FH-CDMA and hybrid systems are presented.

Subsection 5 describes a special data detection method in CDMA systems called Multiuser-Detection, which uses the a-priori knowledge about the code sequences of other users in conjunction with the channel state information. Three different detection algorithms were analysed: Joint Detection CDMA, Joint Parameter Estimation with Data Detection and Interference Cancellation.

A further enhancement of the system capacity can be obtained by combining the advantages of both TDMA and CDMA and such Hybrid TDMA/CDMA systems are discussed in subsection 6.

Multicarrier systems are analysed in subsection 7 which concentrates on OFDM and combinations of OFDM with CDMA in the frequency and time domains. The final subsection deals with MAC protocols for radio data transmission.

6.1   Modulation and Channel Coding

L. Delaunay-Ledter, France Telecom/CNET, France (6.1.1, 6.1.4)
E. Casadevall, UPC, Spain (6.1.1)
A. Rodrigues, Instituto Superior Técnico Lisboa, Portugal (6.1.2)
A.F. Molisch, TU Wien, Austria (6.1.3)
J. Fuhl, TU Wien, Austria (6.1.3)

6.1.1   Linear Modulation

M-PSK and M-QAM Modulations

To provide high data rates required in third generation mobile systems, the use of bandwidth efficient linear modulation could become necessary even if linear amplifier or linearisation techniques have to be added.

The performance of binary phase shift keying (BPSK) with convolutional coding and antenna diversity was analysed. It was shown that partial interleaving strongly degrades the performance in a Rayleigh channel with low Doppler shift in comparison with ideal interleaving, assuming perfect decorrelation of the fading. As an illustration, the ITU-T recommendation G.173 [1] has limited the mean one-way propagation time of public land mobile networks (PLMN) to 40 ms and as a consequence of this, the interleaving depth might be reduced to 10 ms. Coding gains obtained for a rate 1/2 convolutional code of constraint length 5 with a 10 ms partial block interleaver and differential BPSK are given in Tab. 6.1.

	no diversity	2nd-order diversity	4th-order diversity
$f_d \cdot T_s = 10^{-4}$	no	no	no
$f_d \cdot T_s = 10^{-3}$	no	0.8 dB	no
$f_d \cdot T_s = 10^{-2}$	12 dB	6.8 dB	3.2 dB
(ideal interleaver)	(17 dB)	(8.2 dB)	(3.8 dB)

Table 6.1: Coding gains for rate 1/2 convolutional coding with 10 ms partial block interleaving in dependence on different normalised Doppler frequencies $f_d \cdot T_s$ and diversity-orders; transmission rate $R_b = 32$ kbit/s (BPSK); carrier frequency 1.8 GHz

Simulations were also carried out with slow frequency hopping using a 1/3 rate Reed Solomon (6,2) code or a repetition code with interleaving and coherent demodulation in an indoor channel environment, (the power delay profile is modelled as a double Poisson process, [2]). In hopping over 6 frequencies, a normalised frequency separation $S_f \tau_{rms}$ (τ_{rms} for root-mean-square delay spread) larger than 0.1 and 0.2 for the

Reed Solomon code and the repetition code respectively does not improve the performance significantly. On the other hand, for $S_f \tau_{rms}$ larger than 0.05, Reed Solomon codes are more efficient than repetition codes.

Moreover, the cellular mobile radio impairments, (multi-path fading, shadowing, large-scale path loss, [3], and interferer signals), have been considered with a coherent BPSK receiver. For micro (Ricean channel), and macro (Rayleigh) cellular networks, it was shown that at high signal–to–interference ratios (C/I > 20 dB), shadowing affects the bit error rate (BER) less than the Ricean factor within the usual range of these parameters (less than 12 dB of shadowing and Ricean factor between 0 and 1000). The average bit error rate is given in [4].

Assuming a small frequency selectivity, the approximate irreducible bit error rate for multi-level PSK modulation was analysed in [5] with the result that 4-PSK is most robust in Rayleigh channels. In addition, the performance of multi-level quadratur amplitude modulation (M-QAM) in an indoor environment was studied based on a channel model that was determined by a ray-tracing technique. A rectangular pulse shape of length twice the bit period was used, independent of the modulation level. Considering a normalised signal–to–noise (SNR) ratio of 21 dB (irreducible error floor of 10^{-8}), the data rate may be increased from about 10 Mbit/s for 4–QAM, to 23 Mbit/s for 16–QAM, and 29 Mbit/s for 64–QAM with the same bandwidth being occupied.

Further work was done on $\pi/4$–QPSK which is a trade-off between linear and constant envelope modulation.

Transmitter Linearisation

In order to decrease the power spectrum spreading of a linear modulation passed through a class AB, B or C power amplifier, several classical linearising techniques for power amplifiers have been proposed in the literature categorized as: feedforward, feedback, predistortion and LINC (Linear Amplification with Nonlinear Components) transmitter. Among them, the two most promising have been analysed: the predistortion and the LINC transmitters.

In the predistortion technique, the original baseband signal is first predistorted to compensate the amplifier nonlinearity by using a look-up table which could be updated by feedback information. One way to configure the look-up table is to map both inphase and quadrature into an output signal vector. It is also possible to use only one dimensional tables since the distortion in the power amplifier is essentially caused by input amplitude variations. The predistortion using one dimensional look-up tables has appeared more suitable for low data rate systems because of its faster convergence.

The basic principle of the LINC transmitter is to represent any arbitrary bandpass signal, which may have both amplitude and phase variation, by means of two signals which are of constant amplitude and only have phase variations [6]. These two angle modulated signals can be amplified seperately by using class C,D,E or S amplifiers that provide enough power. Finally, the amplified signals are passively combined to

produce an amplitude modulated signal.

Even using the highly non-linear classes C, D, E or S power amplifiers, if perfect balance between both RF branches is assumed, the system is able to obtain a performance as good as that obtained with an ideal linear amplifier. However, in a practical LINC transmitter there are several mechanisms that degrade the overall performance, e.g. the power gain and delay (or phase) imbalances between the two RF paths that cause imperfect generation of the constant amplitude phase modulated signal component. Some theoretical [6] and practical [7] works have been addressed to characterise the impact of these circuit malfunctions on the system performance and so an upper bound on the adjacent channel rejection U_r (ratio between the power in the useful channel with respect to the power in the adjacent channel) has been derived from the gain imbalance ΔG (in dB), the phase imbalance Δf (in degrees), and the normalised guard band between adjacent channels ($\Delta B_g T$), see Tab. 6.2

4–QAM	$U_r[\text{dB}] \geq 32.5 - 19.2\log_{10}(\Delta G) + 5(\Delta B_g T)$
	$U_r(\text{dB}) \geq 48.0 - 20.5\log_{10}(\Delta f) + 5(\Delta B_g T)$
16–QAM	$U_r[\text{dB}] \geq 32.0 - 19.0\log_{10}(\Delta G) + 7(\Delta B_g T)$
	$U_r(\text{dB}) \geq 45.4 - 20.75\log_{10}(\Delta f) + 7(\Delta B_g T)$
64–QAM	$U_r[\text{dB}] \geq 28.5 - 19.0\log_{10}(\Delta G) + 7(\Delta B_g T)$
	$U_r[\text{dB}] \geq 44.5 - 21.2\log_{10}(\Delta f) + 7(\Delta B_g T)$

Table 6.2: Upper bound of the channel rejection with a maximum error of 3dB

The effects of these imbalances on the bit error probability have been analysed, too. In order to emphasise the influence of the imbalances, a system free of intersymbol interference has been assumed. Whereas 4–QAM and 16–QAM modulations remain more or less insensitive to imbalance effects, the 64–QAM and higher order modulations are very sensitive and careful implementations of the RF part are requested when real LINC transmitters are assumed.

In order to evaluate the degradation in terms of BER induced by gain and phase imbalances in a realistic system, the dependence of the BER on the signal–to–noise ratio is shown in Fig. 6.1 and 6.2 for a typical urban environment using a class AB amplifier. A bit rate of 500 kbit/s and a 16–QAM modulation scheme have been considered. As shown in Fig. 6.1, the gain imbalance has to be lower than 0.5 dB to assure no significant performance degradation.

Therefore, although the application of the LINC transmitter is very promising when linear power amplification is required, an imperfect implementation causes an important degradation of the system performance that can completely invalidate the system design, and correction techniques have to be added.
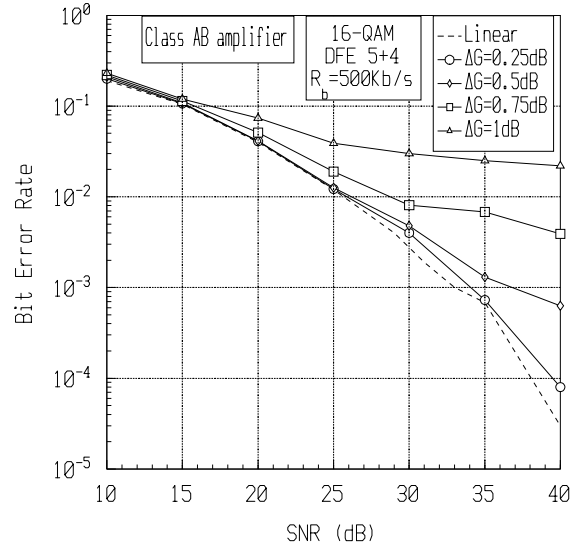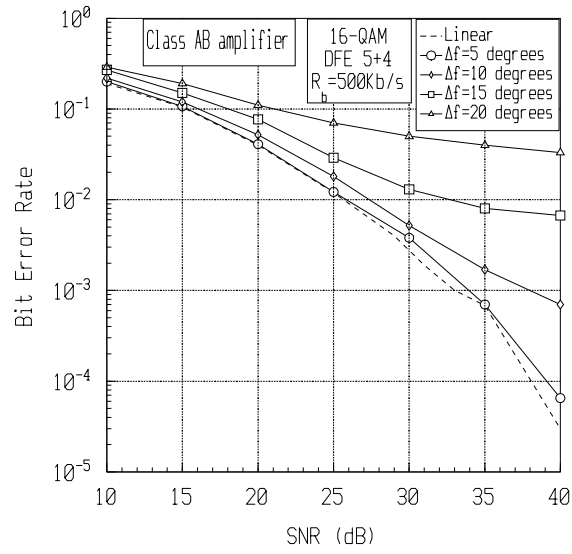
Figure 6.1: Effect of gain imbalances

Figure 6.2: Effect of phase imbalances

6.1.2   Continuous Phase Modulation

MSK and GMSK

Constant envelope phase modulations are currently chosen in mobile radio systems for their ability to support non-linearities in the propagation channel as well as for their good spectral efficiencies and error performances.

The Gaussian minimum-shift keying (GMSK) signal can be efficiently received using a simple MSK-type linear coherent receiver with an appropriate phase detector for the adaptation of a decision directed phase-locked loop. Simulations were performed for different values of phase offset (0 to 15 degrees) and showed that the performance of coherent GMSK with a time–bandwidth product $BT = 0.5$ is almost identical (less than 1 dB degradation) to that of coherent MSK in an additive white Gaussian noise (AWGN) channel [8].

Although the index value 0.5 is needed for coherent demodulation, this choice is not optimum for a limiter discriminator detection. A joint optimisation of modulation index, filters and carrier spacing was done in the AWGN and the minimum bit error rate was achieved for a modulation index of the order of 0.6, with corresponding optimised filters for a C/I ratio equal to 25 dB. Performance in a flat Rayleigh fading channel with or without interference was also evaluated for the modulation index 0.5 and a normalised Gaussian filter bandwidth of 0.3 and 0.5. Using a pre-discriminator filter in the receiver, the required C/I ratio at BER=10^{-3} is 27 dB for $BT = 0.5$ and 27.5 dB for $BT = 0.3$, respectively.

The study of rate 1/2 convolutionally encoded tamed frequency modulation (TFM) [9] with RSSE (Reduced State Sequence Estimation [10]) reception was performed in [11] assuming an AWGN channel. The system optimisation problem was reformulated in order to include the hardware complexity of the receiver, introducing the concept of the "optimum transmitter" under a given receiver complexity constraint. The result show that with an appropriately selected suboptimal receiver an additional coding gain in the order of 0.6-1.2 dB can be achieved compared to uncoded TFM detection.

QMSK and MAQMSK

In order to obtain a better spectral compactness than that obtained with MSK and GMSK, quadratur minimum-shift keying (QMSK) modulation [14] can be used. In comparison with MSK this scheme increases the signal dimensions by a factor of 4 which allows a better spectral efficiency especially if the scheme is combined with multi–amplitude input signals. These multi–amplitude signals are called MAMSK and MAQMSK respectively and their phase diagrams are depicted in Fig. 6.3.

A simple method of calculating the power spectral density permits the comparison of different modulation schemes. Among the different modulation schemes considered, MSK is shown to have better spectral performance than QPSK or QMSK which performed alike. When considering multi–amplitude schemes MAMSK has the most compact performance in comparison with MAQMSK and MSK schemes [15].
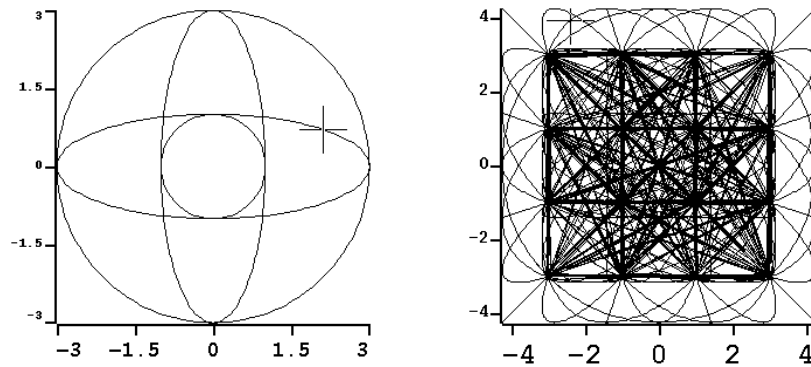
Figure 6.3: MAMSK and MAQMSK signal constellation diagrams

The performance of the QMSK signal was investigated in additive white Gaussian noise and in fast Rayleigh fading channels also considering Doppler frequency shifts and co-channel interference but without considering the existence of multipath. In a AWGN channel and in Rayleigh fading channels with co–channel interference QMSK performs better than GMSK and $\pi/4$–QPSK showing that it is a more resistant scheme in a co-channel interference limited environment (see Fig. 6.4).
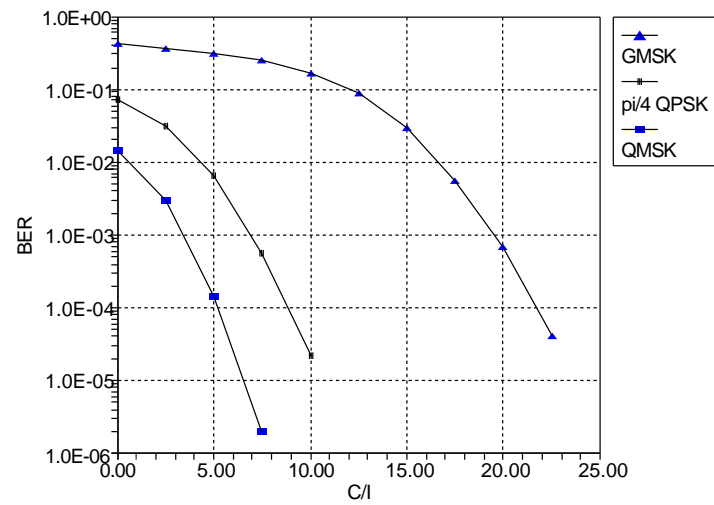
Figure 6.4: Performance of QMSK, GMSK and $\pi/4$–QPSK signal in Rayleigh fading channel with cochannel interference

However, when Doppler shifts are considered the QMSK scheme shows a greater sensitivity to these shifts than GMSK or $\pi/4$–QPSK [15].

Multi-h CPM

As an alternative to the use of single modulation index schemes like MSK or GMSK, multi modulation index schemes (multi-h) [16] were also considered. For a two–path channel model (static two–path) with AWGN, the signature areas of a 2-h CPM scheme were computed as a function of the relative delay of the second path and these were compared with that obtained for 16–, 64– and 256–QAM modulation. Results presented in Fig. 6.5 show the CPM scheme to be less sensitive to interference than the QAM schemes for the same source bit rate and for constant channel bandwidth even when the different bandwidth efficiencies of the CPM and QAM schemes are considered. All the schemes present a maximum of sensitivity for a value of the relative delay between 0.05 and 0.6 times the symbol period [17].
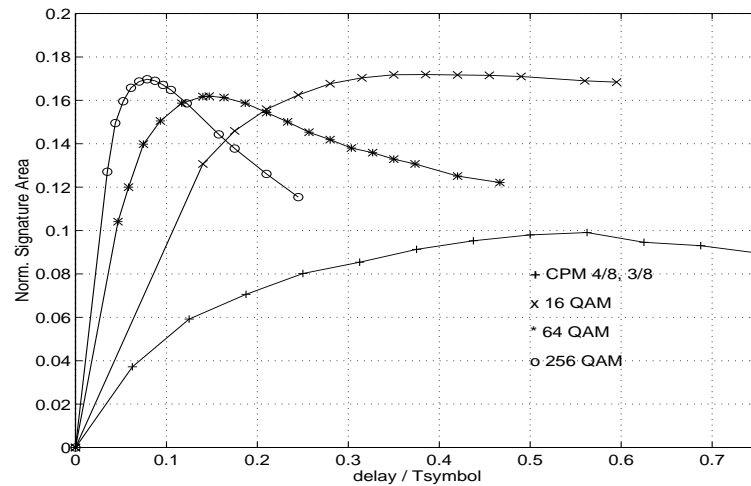

Figure 6.5: Comparison of the signature areas for constant bandwidth as a function of τ/T_{symbol} compensated for the different bandwidth efficiencies

Multi-h CPM modulation schemes are more spectral efficient than GMSK. An analysis of the performance of 2-h CPM was performed for both typical urban and hilly terrain COST 207 channel models [18]. The use of a post-detection diversity (PD) scheme implemented by means of two Viterbi receivers was also considered allowing further performance improvements.

Also a combination of a multi-h CPM modulation with a direct sequence spread spectrum system and its performance in several indoor environments was investigated.

Three different channels were analysed: line-of-sight, non line-of-sight and large buildings with maximum delay spreads of 100, 200 and 400 ns, respectively [19]. Results are given for two different multi-h codes considering a coherent receiver structure and two types of diversity: selection diversity (SD) and post-detection diversity. Results in Fig. 6.6 indicate that multi-h spread spectrum systems can achieve good performances in indoor environments for relatively high data rates (1 Mchip/s) but the use of diversity is essential to achieve an acceptable BER with realistic E_b/N_0, specially in large buildings [20, 21].
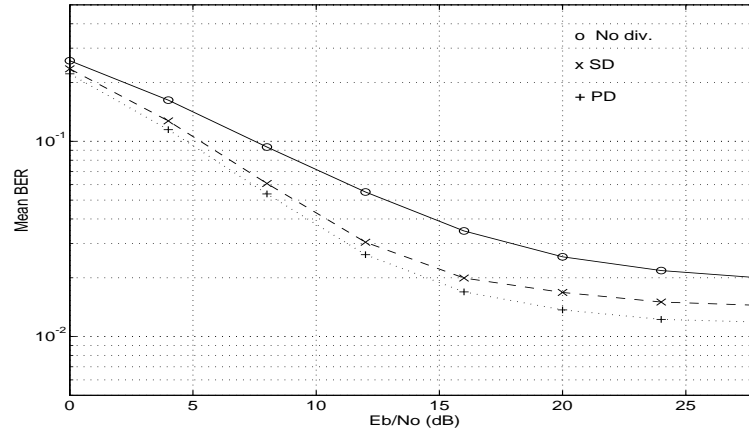

Figure 6.6: Error performance of coherent multi-h CPM ($h_1 = 2/4; h_2 = 3/4$) in a an urban area (large buildings) without diversity, with selection div. (SD) and post-detection div. (PD)

A comparison between multi-h CPM and CPFSK (continuous phase frequency shift keying) was also made for AWGN channels using the concept of equivalent minimum distance for non-coherent detection. Multi-h signals maintain their superiority over CPFSK in the case of non-coherent detection with gains up to 2.28 dB. The performance of the non-coherent receiver can be as good as the coherent one for certain values of the modulation index and for long observation intervals in the receiver (greater than 100 symbol periods) [22].

6.1.3 Performance of MSK in time dispersive channels

The time dispersion of the mobile radio channel causes intersymbol interference (ISI) that results in an irreducible BER usually called error floor. The error floor constitutes the performance limit for a given channel and a modulation/detection scheme (without

equalisation). For cordless phones, the cost and system complexity must be kept low so they usually have no equalisers. Furthermore, the SNR in indoor scenarios is high, so the error floor is a quite good performance measure. In Chapter 5 (DECT), the results and practical applications are described. In this section, we concentrate on the basic mathematical methods. For the case of differentially detected pure MSK with fixed sampling and delay spreads that are small compared to the bit length, various computation methods have been developed:

The group delay method [23, 24] — The differential detector decides that a "1" was transmitted if the phase difference between two adjacent samples lies between 0 and π, and a "-1" was transmitted if the phase difference lies between π and 2π. Without time dispersion, the phase difference is $\pi/2$ or $3\pi/2$, respectively. The differential detector thus makes an error if the phase error introduced by the (instantaneous) group delay lies between $\pi/2$ and $3\pi/2$. Averaging over the statistics of the group delay [25] we get an approximate equation for the BER: $\text{BER} = (1/2)(S/T)^2$. Here, S is the mean delay spread and T is the bit length. Closer inspection of the error mechanisms show that group delay bursts occur when the amplitude of the received signal becomes very small, i.e. in deep fades.

The error region method [26, 27] — This method is described in Chapter 5, since it is also suitable for adaptive sampling, and thus can be readily applied to DECT systems.

The echo method [28] — For the echo method, we interpret the (general) impulse response, as a sequence of echoes, where each echo has its amplitude A_i and phase ϕ_i. Using the Gaussian WSSUS model and the assumption of a slowly varying channel, the A_i are (known) constants, while the ϕ_i are uniformly distributed statistical variables. We can then compute the total phase for a certain input sequence and determine for which ϕ_i errors occur. Averaging over the statistics of the ϕ_i, we finally arrive at the error probability.

All three methods have some restrictions: the group delay method gives only approximate results and is only applicable if the delay spread is much smaller than the symbol length, sampling is done on the average mean delay, and we have no LOS component. The error region method is essentially restricted to the two–delay channel but works also for LOS, larger delay spreads, and arbitrary sampling time. The echo method requires that we have no LOS components and that $S \ll T$, but works for general impulse responses and arbitrary sampling times. In none of these methods noise is included.
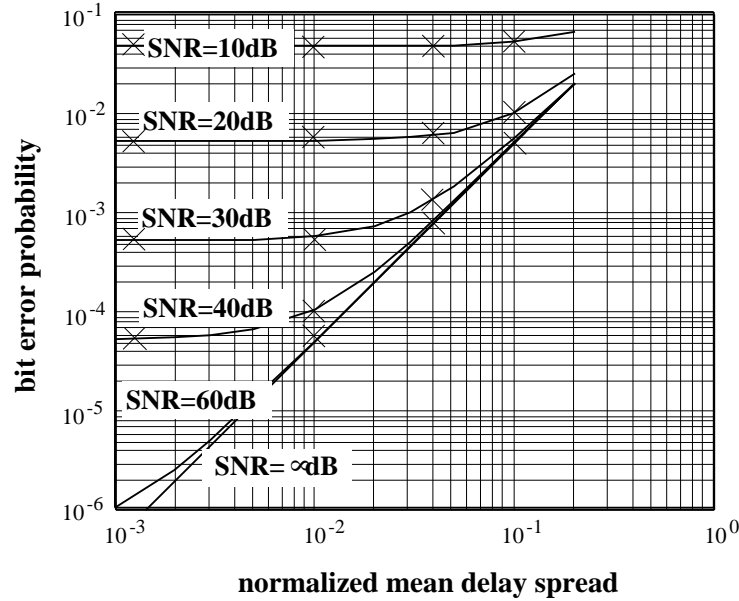
Figure 6.7: Error probability of MSK in a 10–path fading channel

The correlation matrix method [29] — A fourth method, the so–called "correlation matrix method", lifts these restrictions. It can be shown that the real and imaginary parts of the received signal at two subsequent samples are Gaussian variables, whose correlation matrix can be determined from the average channel parameters and the modulation format. The BER is then the probability that a certain combination of these samples fulfills an error condition. Several methods for the evaluation of this probability exist: direct numerical evaluation, approximation methods for small error probabilities, and construction of an "equivalent" two–path model that has the same correlation matrix, and thus the same error probability.

The second case of interest are outdoor scenarios, especially in the context with GSM (see Chapter 5). For typical delay power profiles, the duration of the impulse response is larger than the bit length. In that case, the approximate BER can be computed for sampling at the shortest excess delay. The mean power of the current bit is $P_b = \int_0^T P(t)\,dt$ and the power of the interfering bits is $P_h = \int_T^\infty P(t)\,dt$. It was shown [30] that the average BER is approximately BER $= [2(1 + 2P_r)]^{-1}$, where $P_r = P_b/P_h$. This equation is also valid in indoor scenarios for very high data rates. Such high data rates are possible if a strong LOS component is present; e.g. for a 10 dB LOS and 2-PSK, 20 Mbit/s are possible. For non–LOS, the BER with fixed sampling and 100 ns delay spread is in the order of 10^{-2} for bit rates of 1 Mbit/s.

6.1.4 Trellis Coded Modulation (TCM)

TCM represents an attractive solution to improve performance for mobile radio transmission without extra bandwidth requirements. Two different concepts of TCM exist, one based on the Ungerboeck method [31] with one convolutional code, other based on the Imai method [32] where the partition levels are encoded with several binary codes.

A new criterion for designing the Imai code for a Rayleigh channel was proposed, derived from the Sundberg's approach, [33]. The main difference was to use sub–codes with unequal Hamming distances, chosen to optimise the coding gain at a specific bit error rate. The optimised solutions for a 10^{-3} bit error rate in a Rayleigh channel are given in Tab. 6.3, [34].

rate (bit/symbol)	Modulation	code	required E_b/N_0 (dB)
0.5	4–PSK	1/4	3.5
1		1/2	5.1
1.5		3/4	9.2
2	8–PSK	3/8,3/4,7/8	11.5
2.667	16–PSK	1/4,2/3,5/6,11/12	13.1
3.167		1/2,4/5,11/12,11/12	16.7

Table 6.3: Summary of code rates and required E_b/N_0 for BER=10^{-3} (Rayleigh fading channel)

However, whatever the access technique may be, partial interleaving has an influence on coding efficiency and therefore on TCM performance. A modified Chernoff bound taking into account the effect of correlated fadings can be found in [35]. This point has been illustrated for coded 8-PSK with code rate 2/3. The simulation results reported in Tab. 6.4 refer to a 64 kbit/s data rate in a Rayleigh channel considering pedestrian and vehicle speed by a 10 ms interleaver delay.

BER	perfect interleaving	v=190km/h	v=40km/h	v=4km/h
10^{-2}	6 dB	4.6 dB	2.1 dB	0.5 dB
10^{-3}	12.5 dB	10.6 dB	7.3 dB	4.6 dB

Table 6.4: Coding gains of trellis coded 8-PSK compared to uncoded QPSK; R_b=64 kbit/s; 32×10 block interleaver; f_0=1800 MHz

Frequency hopping techniques can provide the way to make the interleaving process

more effective. In particular, the effect of frequency hopping was analysed for eight-states trellis coded 8–DPSK taking into account the correlation among the different frequency channels involved. In each channel flat fading was assumed with a maximum Doppler frequency of 5 Hz. The correlation of the complex channel transfer function $H_c(f, t)$ versus the frequency separation S_f was assumed to be

$$E\left[H_c^*(f, t)H_c(f + S_f, t)\right] = \frac{1}{1 + j2\pi S_f \tau_{rms}}$$

resulting from an exponentially decreasing power delay profile with rms delay spread τ_{rms}. A block interleaver of order $N_L \times N_C$ was considered, and the N_L formed slots were modulated according to N_L assigned hopping frequencies. As shown in Fig. 6.8 for $S_f \tau_{rms}$ smaller than 0.15, the degradation of performance with respect to the uncorrelated case becomes significant. The uncorrelated results can be found in [9].
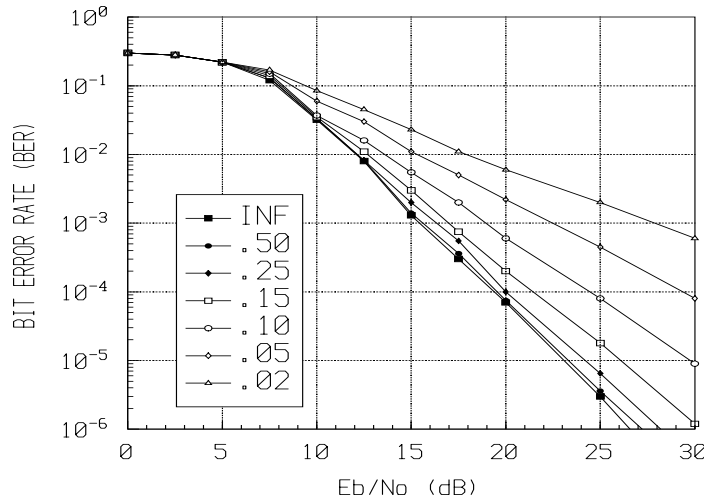

Figure 6.8: Bit error rate for FH-TCM-8DPSK with normalised frequency hopping separation as parameter

The two–branch post–detection diversity solution to combat the Rayleigh fading has been also investigated with perfect interleaving assumption. At a BER of 10^{-3}, post-detection selection, equal gain combining (EGC) and maximal ratio combining (MRC) diversity techniques have offered a relative coding gain over the eight-states trellis coded 8–DPSK (rate 2/3) without diversity of approximately 5.9, 6.2 and 6.6 dB respectively. Additional results have also pointed out that TCM with diversity is more robust than TCM without diversity regarding the effects of co-channel interference.

The primary interest of TCM for a mobile system is its bandwidth efficiency. As described in [36], the spectrum efficiency η of a cellular mobile system depends on the C/I ratio, on modulation parameters, and on propagation characteristics as cell radius and propagation loss factor α. As shown in Tab. 6.5, the system efficiency in a macro cellular environment can be greatly improved by using a coded 16–QAM modulation (16 states 2/4 code built from two one–dimensional TCM schemes) instead of uncoded 4–QAM.

	$\alpha = 4$	$\alpha = 6$	$\alpha = 8$
$\dfrac{\eta(\text{TCM})}{\eta(\text{4-QAM})}$	5.61	3.15	2.37
$\dfrac{\eta(\text{TCM})}{\eta(\text{16-QAM})}$	6.3	2.7	1.77

Table 6.5: Spectrum efficiency in a cellular network

6.2   Equalization

G. Kandus, Institute Jozef Stefan, Slovenia (6.2.1)
L. Delaunay-Ledter, France Telecom/CNET, France (6.2.2)
E. Casadevall, UPC, Spain (6.2.3)

Equalisation techniques with or without an adaptive component can be added to combat the degrading effects of multipath propagation on wideband single carrier transmission systems.

6.2.1   Convergence of classical adaptive algorithms

The convergence properties of adaptive algorithms such as the gradient, conjugate gradient (CG), least mean square (LMS) and recursive least square (RLS), and the conditions for their stability have been studied. It was shown that both the gradient algorithms and the LMS algorithm converge slowly, requiring many iterations. The RLS algorithm gives a better performance than the LMS algorithm at the cost of increased computational complexity. The RLS algorithm requires N^3 iterations (N=number of filter coefficients) or N^2 in a modified form whereas the CG algorithm requires only N iterations. None of these first order methods could compare with the optimum Kalman filtering method. Finally, the implementation of parallel algorithms was suggested to improve the rate of convergence.

The fast adaptive, zero order conjugate algorithm, used to find the optimal weights for an adaptive filtering process by minimising the sum of squares of non-linear functions, has also been studied in detail. The method could be applied to personal mobile systems if the number of adaptive filter coefficients is less than 12.

6.2.2   Advanced Equaliser Techniques

The first investigations on equaliser techniques concentrated on reducing the complexity of the well known Viterbi equaliser. The sub-optimal decision-feedback sequence estimation (DFSE) algorithm allows a higher transmission rate with only a small performance degradation [37]. In most cases, prefiltering prior to the DFSE leads to an additional performance gain [38]. Numerical results with COST207 multipath channels are given in subsection 6.2.3 [39].
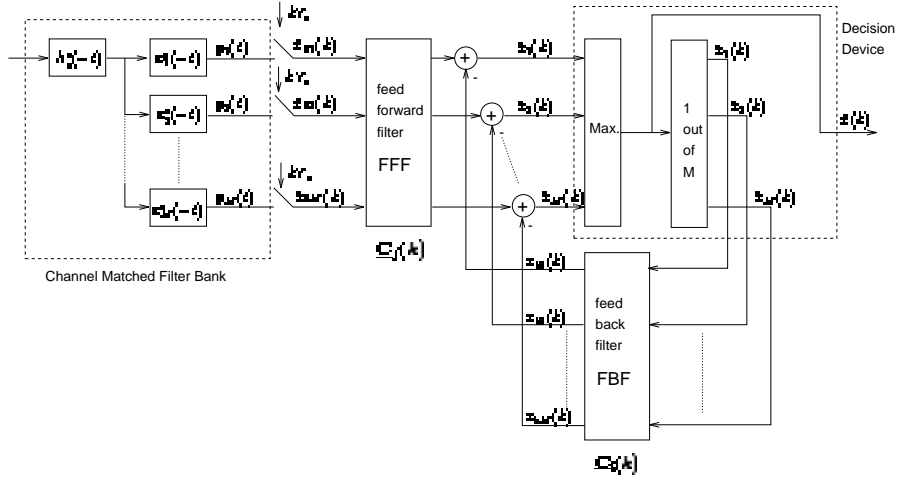
Figure 6.9: Structure of a vector decision-feedback equaliser for M-ary orthogonal signals

When transmitting over fast fading channels, the information symbols are usually arranged in blocks separated by known symbols as in the GSM system. The zero-forcing decision-feedback equaliser (ZF-DFE) has been adapted to such a scheme leading to the zero-forcing block-decision-feedback equaliser (ZF-BDFE).

In addition, the vector decision-feedback equaliser (VDFE) known from multi–user detection techniques has been applied to a single user system with M–ary orthogonal modulation, [40], see Fig. 6.9. Compared to a conventional receiver for orthogonal modulation, the selection device has been replaced by the VDFE where the input and output signals are vectors. Consequently, the feedforward and feedback filters are matrix FIR filters. As shown in Fig. 6.10, in a two-path channel significant performance gains have been obtained using the VDFE. Although the VDFE has been designed for a single user system with M-ary orthogonal modulation, it can be used as a first stage of a multi-stage multi-user detector, each user using a different codeset, e.g. Walsh-Hadamard codes like in the Qualcomm CDMA system (IS-95).

Finally, the neural network equaliser concept has been evaluated for an indoor radio channel and compared to the traditional linear transversal equaliser structure. The performance has been evaluated for the Multilayer Perceptron (MLP) with 2– and 4–PSK modulation. But the performance gain obtained by the MLP is too small to justify its additional complexity.

6.2.3 Joint diversity and equalisation Techniques

The diversity concept can be included in the equalisation procedure to improve the system performance. Two major equalisation techniques have been studied, Maximum
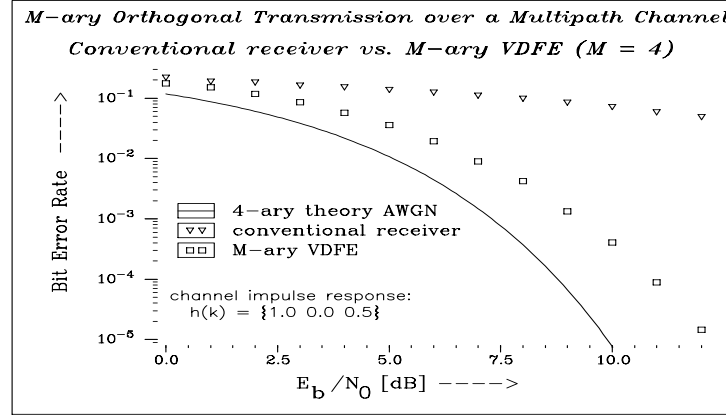
Figure 6.10: Performance of vector decision-feedback equalisation using a two path channel model

Likelihood Sequence Estimation (MLSE) and Decision Feedback Estimation (DFE).

Maximum Likelihood Sequence Estimation

Two solutions applied to the DFSE algorithm have been suggested: combining/selection at sample level, i.e. the signals received in different diversity channels have to be combined before equalisation and combining/selection at the metric level, i.e. the metrics used in the Viterbi algorithm have to be modified (in the combining technique, the partial metric on the Viterbi algorithm trellis is calculated as the sum of metrics from each diversity channel, and in the selection technique, the channel with the higher power level is selected).

Fig. 6.11 shows the simulation results obtained for various receiver structures for a transmission over the HT50 COST207 channel. GMSK modulation and a 4–state trellis with metrics evaluated as proposed in [41], [42] were used.

Of the receivers tested, the DFSE operating with combining at the metric level provides the best performance. However, the structure with selection at the sample level seems to be more suitable because of its lower complexity for only 2dB loss.

Decision Feedback Equaliser

The performance of the joint diversity and DFE equalisation techniques was analysed for the 4–QAM modulation and the variation of the BER with the normalised delay spread $\tau_{rms}R_b$, where R_b denotes the bit rate, was considered. As shown in Fig. 6.12, the BER values with diversity can be decreased by an order of magnitude if the channel introduces low distortion. When equalisation is added to cope with the ISI, the system
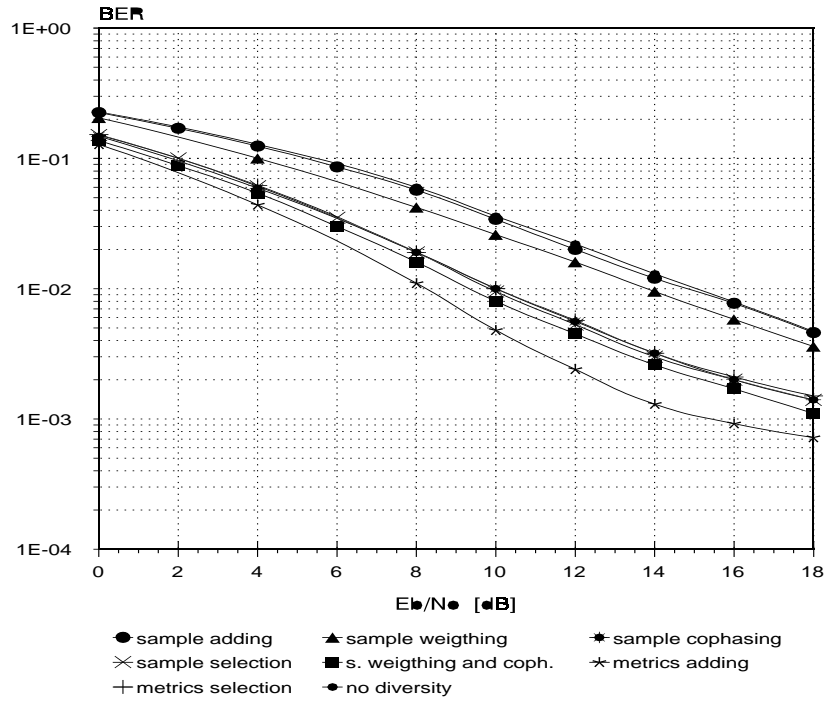
Figure 6.11: Performance of DFSE with diversity in the HT50 channel

is able to maintain a similar performance for high values of $\tau_{rms}R_b$ when compared to the performance obtained in frequency-non-selective channel. On the other hand, with joint diversity and equalisation techniques, the system performance improves approximately by two orders of magnitude when compared to the use of equalisation alone. No advantage in terms of maximum transmit data rate has been found with 16–QAM modulation [43].

The influence of the impulse response correlation between both diversity branches was analysed, too. If the correlation between these two branches in a Rayleigh channel with normalised delay spread $\tau_{rms}R_b = 1$ is lower than 0.5 the system performance shows no more improvements.

Finally, the use of a micro-diversity technique for the mobile and portable set could substantially improve the system performance with no prohibitive increase in complexity.
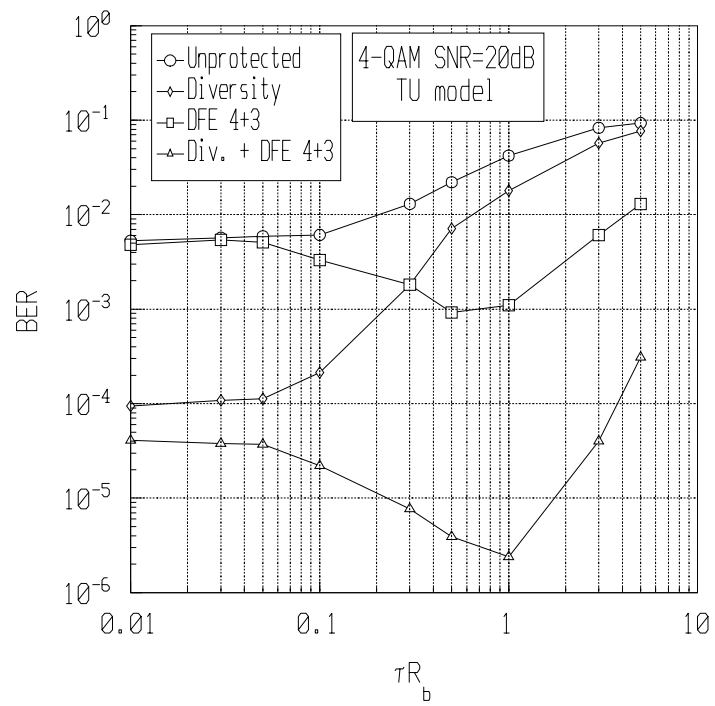
Figure 6.12: Performance of joint diversity and DFE equalisation as a function of the normalized delay spread

6.3   Enhanced TDMA

A. Burr, University of York, United Kingdom

6.3.1   TDMA enhancements

Consideration of possible enhancements to TDMA systems neccessarily involves a number of concepts that are dealt with in much more detail elsewhere in this report. The object of this section is to describe how these concepts may enhance the performance of TDMA systems. Therefore to avoid excessive overlap we will cover here only the influence of these areas on TDMA performance specifically.

Coding and coded modulation

The development of enhanced coding and coded modulation techniques and their application to mobile and personal communication systems has been considered in section 6. However, it has been shown that the application of FEC coding and coded modulation can enhance the capacity of a cellular system significantly. In TDMA systems, it allows much reduced re–use distances, and hence increased re–use factors. Second generation digital systems such as GSM and IS–54 in general make use of coding only for special purposes, such as to protect class I speech bits. Hence there are enhancements possible in an advanced third generation TDMA system by this means.

Both FEC coding and coded modulation are used in the ATDMA adaptive transport architecture. A "toolkit" consisting of a range of both modulation and coding techniques, including a coded modulation scheme [44], is available for use where channel conditions and service requirements warrant it. More details are given in chapter 7. The improvement from the use of coded modulation has been evaluated at about 4 dB, when used in conjunction with DFE on a Hilly Terrain channel model with ideal interleaving. This may allow a reduction in cluster size.

A range of FEC codes are also available in the coding "toolkit". These are concatenated codes based on a 1/2 rate convolutional inner code and an extended Reed–Solomon outer code, which may be punctured to increase its rate. A range of rates between 3/4 and 1/4 is available by this means. Again, more details are given in chapter 7. Special care is required for speech services to remain within the delay budget. For these services interleaving depth is restricted to 4.

It has been shown by means of simulation that in general the use of FEC can increase capacity by a factor of nearly two on an AWGN channel, and by more than four on a Rayleigh fading channel. It also allows 100% re–use, even in TDMA systems, which both increases capacity and removes the need for frequency planning. The spectral efficiencies of these schemes are compared in Table 6.6.

Adaptive modulation and coding

Adaptivity has been identified as the most effective means of enhancing a TDMA system for the third generation [45, 46, 47]. There are two reasons for this: firstly, a third generation system must accommodate a very wide range of services and channel types, from pico- to macrocellular, and for data rates up to 2 Mbit/s. It is clear that no one air interface can be optimal for all these conditions. Secondly, it has been shown that such adaptivity can increase the average capacity of a cellular system by several times. Conventional TDMA cellular systems must be designed for the worst case, which will lead in most cases to an air interface which is substantially over–specified. Allowing adaptation to the actual channel conditions can result in much more efficient use of resources on average.

The system may adapt to a range of factors related to both the channel and service. On the most fundamental level a different air interface is likely to be required in different cell types, and for different services (whether speech or data, data rate, BER and delay requirements). In addition, it may take into account the current characteristics of the channel, such as fading conditions, delay spread, and co–channel interference. For example, the delay spread is likely to limit the maximum symbol rate used. Adaptation may apply to the modulation scheme and signalling constellation and to the FEC coding scheme, among other system features.

Adaptive modulation and coding is a major feature of the ATDMA system. Fig. 6.13. shows the architecture of the ATDMA adaptive transport interface, showing the features that can be adapted and the range of measurements on which the adaptation is based.

In addition, the effect of adapting the modulation/coding to co–channel interference in a non–fading channel has been considered. Fig. 6.14 shows how this gives rise to an improvement. In a conventional TDMA system, the coding must be chosen so that communication at a sufficient quality is provided for the proportion of cases specified by the availability requirement (as shown). This constrains the choice of code and hence the spectral efficiency. In an adaptive system, however, the code can be chosen according to the actual signal–to–interference ratio encountered. Note, too, that because the spectral efficiency of the codes increases more rapidly than linearly with signal to noise ratio, the efficiency of the adaptive scheme is greater than that of a CDMA scheme, which because of interferer diversity operates at near the average signal to interference ratio.

PRMA

A form of statistical multiplexing is available in speech transmission systems by taking advantage of the voice activity factor, defined as the proportion of the time a link in a full duplex speech connection is actually occupied by a speech signal, and is usually taken as about 0.4. This effect is widely quoted as an advantage of CDMA over TDMA, since in a CDMA system advantage can be taken of it in a particularly simple way by means of voice activation. However, a similar advantage can be obtained
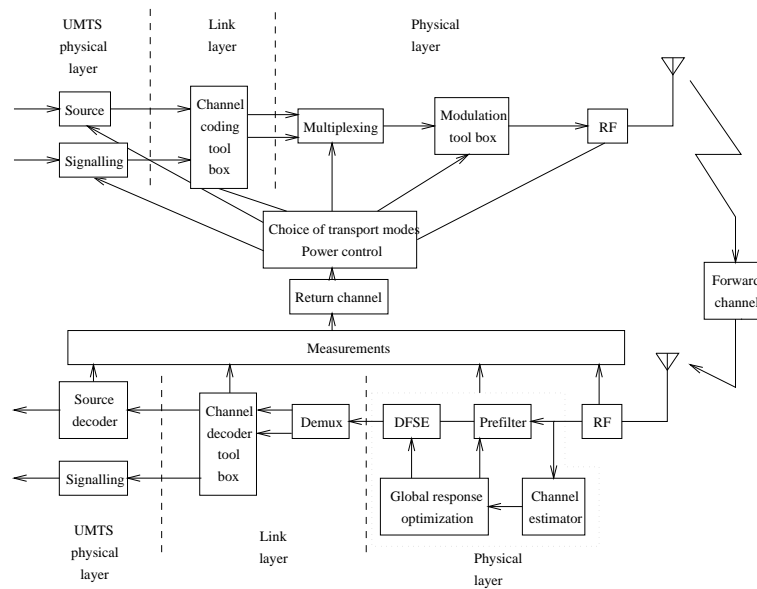
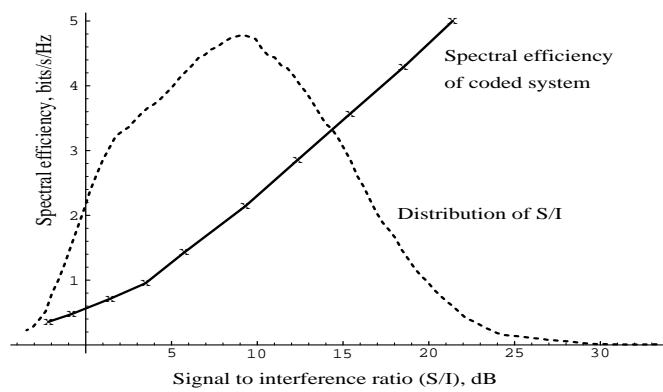Figure 6.13: Architecture of ATDMA adaptive transport interface

Figure 6.14: Spectral efficiency of adaptive TDMA

in TDMA, albeit with higher complexity, using reservation schemes such as Packet Reservation Multiple Access (PRMA).

The capacity of a PRMA system has been evaluated using a Markov model of the channel assignment process [48]. It is assumed that one speech packet may be buffered while waiting for a successful reservation without causing excessive delay. Packets delayed any further than this are dropped. For a TDMA system containing 20 slots, with probability of successful reservation 0.4, it was found that 37 users may be accomodated for a packet dropping probability of less than 1%. Given the voice activity factor of 0.43 assumed in this work, this corresponds to a throughput of 79%.

A more detailed simulation study [49] has evaluated PRMA in a cellular system, taking into account a number of system design options. A distinction is made between packets dropped due to delays arising from unsuccessful contention for a reservation, and due to interference from neighbouring cells. Packet dropping from both sources is to be kept below 1%. The system options considered are as follows:

- Use of additional error protection in packet headers, so that reservation may be held even if information cannot be received (described as "Option 1");

- Use of power control;

- Speech model capable of taking into account "minigaps" in speech activity (described as "fast" as opposed to "slow")

- Cluster size

The results show that "Option 1" does not increase capacity, since normally the packet loss is dominated by interference effects. It is better to allow a reservation to be lost and try again. Power control does help because of the reduction in interference, although it prevents the capture effect in contention. The "fast" speech model in fact degrades capacity because it increases contention, and thus also interference. As expected, capacity per cell increases with increasing cluster size, but overall spectrum efficiency is in fact highest with a cluster size of unity. For cluster size 3 and required C/I threshold of 8 dB a capacity of 32 users/cell is attainable (in an urban area), corresponding to a throughput of 67%. However, the maximum efficiency in users/cell/carrier is 12, for cluster size unity.

A more theoretical analysis of the use of PRMA within an adaptive TDMA system gives a throughput increase of 64% when voice activity is taken into account. The overall throughput is then 66%, but this takes into account also the variation in system capacity due to the use of adaptive coding. Also this assumes only 30 users/cell: larger numbers would allow greater throughput by increasing the statistical multiplexing effect.

A variant of PRMA called PRMA++ is used in the ATDMA system [50], as described in chapter 7. In all cases the base station is in control of the process. A set of random–access channels is used for mobile stations (MS) to request resources. Note that, as in the analysis described in the previous paragraph, the PRMA++ system is also used

with link adaptation, to allocate new resources whenever a change in channel conditions requires new resources. Likewise repeat requests are treated as a new demand for resources.

Dynamic channel allocation

Dynamic channel allocation (DCA) has been described as one of the most important means by which capacity can be increased in third generation TDMA systems, allowing them to compete with CDMA. Dynamic channel assignment schemes allow channels to be allocated to cells according to actual traffic load, rather than according to a fixed re–use plan (described as Fixed Channel Assignment – FCA).

Some DCA schemes of this sort have been compared with FCA. Several schemes are described, the simplest assigning any available channel in the cell and its immediate surrounding cells. More sophisticated schemes assign the channel re–used in the nearest cell site outside the surrounding cells. The results suggest that DCA is superior to FCA, especially when the traffic is non–uniform either in time or space, but for uniform traffic the difference is not large.

A PRMA scheme has been described which also effectively functions as a DCA scheme [49]. Here a channel is assigned to a packet stream on the basis of the interference detected in that channel. Thus channel assignment depends on channel usage at the time of assignment. It has been shown that the greatest capacity is obtained in this system with a cluster size of 1 (i.e. 100% re–use), in which case the scheme is equivalent to full DCA.

Note that adaptation to co–channel interference levels, mentioned in section 6.3.1. above, also has a similar function to dynamic channel assignment, since it can similarly take into account the actual usage of channels in the vicinity of a cell. Further, consideration of coded TDMA suggests that the optimum capacity in coded TDMA systems may be obtained with 100% frequency re–use, thus avoiding frequency–planning altogether.

6.3.2 Capacity comparisons

A great deal of research has compared the performance (in terms, mainly, of capacity per unit bandwidth per cell) of TDMA and CDMA. A wide variety of approaches have been used in this work, from fundamental theoretical bounds to detailed consideration of specific systems, and a wide range of conclusions are reached. The comparison of specific systems will be left to chapter 7. Here we are concerned more with any inherent difference between the multiple access techniques.

An analysis of information–theoretic capacity of TDMA and CDMA systems within a single cell has been performed [51]. The results are given in Fig. 6.15. This shows that on the conventional assumption that other users are treated as noise, binary TDMA capacity ($C_{Bin}, K = 1$) exceeds CDMA capacity (C_{ON}). If, however, other users are not treated as noise, presupposing some form of interference cancellation or joint detection, then CDMA capacity ($C_{Bin}, K = 10$) exceeds binary TDMA. If both TDMA and

CDMA signals have a Gaussian distribution, (and CDMA is jointly–detected), then capacity is equal (C_{Gauss}). For CDMA this indicates that joint detection is desirable; for TDMA that the availability of non–binary modulation schemes is important.
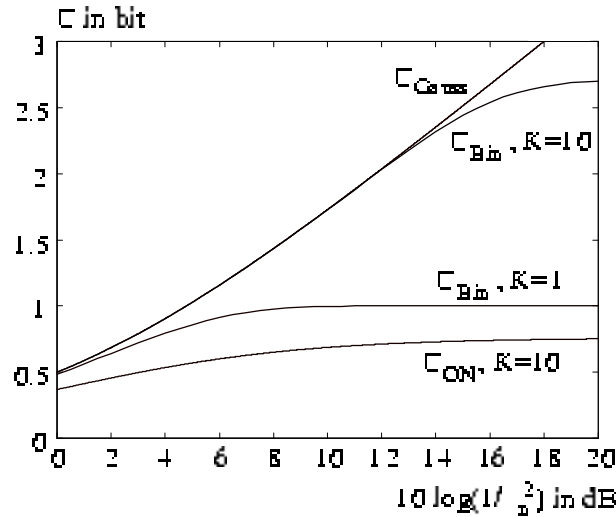

Figure 6.15: Information theoretic capacity of single–cell systems

A generic approach for multicellular systems has been developed [52, 45]. Here an attempt has been made to compare TDMA and CDMA on a equitable basis, assuming that wherever possible features of a CDMA system are also taken into account for the TDMA system. Thus interferer diversity may be included using SFH (see section 6.6.1); power control and voice activation are both included in the TDMA systems; and suitable FEC codes and coded modulation schemes are included, of equivalent power in both systems. Worst–case and average–case analyses have been obtained, but capacities have also been calculated for 95% and 99% availability. The results are given in Table 6.6 , in the form of spectral efficiency in bits/s/Hz/cell–site. In this table "orthogonal CDMA" refers to CDMA schemes in which true orthogonality is achieved, for example frequency–hopping with orthogonal patterns, or decorrelation receivers. "Ideal cancellation" assumes perfect cancellation of all intra–cell inter-ference. The results show that conventional DS–CDMA outperforms TDMA, even with coding. However, it should be noted that PRMA is not used here, and might increase TDMA capacity. Orthogonal CDMA gives a smaller advantage than might be expected, mainly because low rate codes cannot be used in the same way as in DS–CDMA. It will, however, be largely immune to the near–far effect. CDMA with ideal interference cancellation gives the best results, but is not necessarily achieve-able, even with maximum–likelihood multiuser detection. Adaptive TDMA, however,

Scheme	AWGN		Fast fading	
Availability	95%	99%	95%	99%
Uncoded TDMA	0.34	0.19	0.11	0.06
Coded TDMA (cluster size 3)	0.39	0.24	0.28	0.20
Coded TDMA (cluster size 1)	0.60	0.46	0.49	0.39
DS–CDMA	0.72	0.67	0.67	0.62
Orthogonal CDMA	1.19	1.10	0.54	0.49
CDMA with ideal cancellation	1.72	1.51	1.57	1.38
A–TDMA	1.94		1.05	

Table 6.6: Spectral efficiencies (bits/s/Hz/cell) of various multiple access schemes

is very close to it.

6.3.3   Summary

We conclude by noting that there are two main approaches to enhancing the capacity of a TDMA system, which are to a large extent incompatible, as well as a wide range of other techniques that can be used to enhance any system.

The first approach is to invoke the interferer diversity effect, by adding an element of spectrum spreading. This is exemplified by the hybrid systems, considered in section 6.6: TDMA/SFH, JD–CDMA, and CTDMA. These systems also make use of a TDMA element and/or advanced signal processing to eliminate the intra–cell or self–interference which degrades the capacity of conventional CDMA systems. The effect is that each user encounters interference due to a large number of users in co–channel cells, leading to an averaging effect. Thus all users encounter co–channel interference close to the average, and system design can be for the average case, rather than the worst–case interference. Note that this approach also readily benefits from the use of voice activation.

The second approach, exemplified by the ATDMA system, is to adapt to the co–channel interference encountered. Thus more spectrally–efficient modulation/coding can be used when the C/I ratio is high, using fewer resources, with less spectrally–efficient modulation and more powerful coding when the interference level requires it. Thus a larger average capacity is achieved. In principle this may yield a larger capacity than the interferer diversity approach, since a graph of spectral efficiency against C/I is non–linear (Fig. 6.14), such that the average capacity for variable C/I exceeds the capacity achieved at average C/I. However in practice it may be more difficult to implement the more spectrally–efficient modulation schemes required. The approach also lends itself well to the use of PRMA, which also allows voice activity to be taken advantage of quite readily. This approach may be considered as theoretically and potentially more efficient, but also technically more difficult.

6.4   CDMA

P. Hulbert, Roke Manor Research Ltd., United Kingdom

This section covers direct sequence (DS) and frequency hopped (FH) CDMA as well as some work on packet radio technology based on hybrid DS–FH CDMA.

6.4.1   DS-CDMA

A considerable amount of research was conducted on this topic under COST 231, reflecting the high level of international interest. This sub–section has been further sub–divided into six parts. The first four cover design aspects which critically affect capacity or spectral efficiency. The fifth covers detailed evaluations of the resulting capacity. The sixth part covers a key element relating to efficient implementation.

Diversity Receiver Performance in Multipath Conditions

The subsection covers research to evaluate the performance of several Rake receiver architectures with particular modulation schemes and various channel models. One example of antenna diversity evaluation is also included. For each of the evaluations, the radio channel model was based on a tapped delay line with discrete multipath components with random phase and amplitude. The relative levels of the mean tap energies and the progression of the levels and phases with time differed according to the research team.

The work reported by Y. Tanik et al. of METU, Ankara, Turkey related to spread spectrum pulse shaped BPSK modulation. The channel model was based on the work of Hashemi [53], combining experimental data taken at 1280 MHz with 100 ns resolution and spatial resolution of 1 m.

In the Rake receiver the matched–filtered input signal was quadrature–demodulated and sampled at the chip rate. This complex valued sequence was then passed through a tapped delay line whose outputs were de–spread and weighted by the estimated multipath gains of the channel to form a maximal ratio combiner. The path estimates were obtained through a decision feedback mechanism: The despreader outputs were multiplied by the detected bits and low–pass filtered. The cutoff frequency of the lowpass filter (LPF) was assumed to pass Doppler components of the multipath processes.

The BER performance was evaluated both analytically and by simulation producing detailed results. In both cases a Gaussian approximation was made for other user interference. A typical result was a BER of 0.02 for $E_b/N_0 = 6.7$ dB, for a spreading factor of 100. The filtering method of channel estimation was found to produce negligible increase in BER.

Another significant result was that the number of taps could be reduced below that necessary to cover the complete delay spread of the channel without significant performance penalty. In fact coverage of as little as 3 - 4 μs was found to give acceptable performance. But although the input SNR was assumed to be a constant (through

power control) the average BER was observed to vary in a range up to a decade due to fading.

The team at CSELT, Torino, Italy (Palestini, Levi, et al) examined filtered (Root Raised Cosine) spread spectrum DBPSK modulation processed by a Rake receiver which maximal ratio combined the multipath components after differential decoding. The Rake fingers were aligned on a 1 chip "grid". The channel model was based on the COST 207 typical urban channel. The BER performance was evaluated as a function of the number of Rake fingers for 1 and for 5 Mchips/s. It was shown that the optimum number of Rake fingers rose from 6 to 10 in moving to the higher chip rate as more multipath components were resolved.

The same team also extended the evaluation to cover antenna diversity. Essentially, the above model was extended to multiple antennas with various types of combining of the Rake receiver (one for each antenna) outputs. Equal gain combining gave the best performance.

The diversity gain is significantly notable; for example, by considering uncorrelated fading and no channel coding in the one user scenario, at BER=10^{-3} a 6 dB gain was obtained with second order diversity and a further 2.5 dB gain was achieved by adding a third antenna. When channel coding and interleaving were simulated, the gain became 3.5 and 5 dB with 2 and 3 antennas, respectively.

With correlated fading, a certain degradation was introduced, but in comparison to the case where no antenna diversity is applied, a gain was still present due to uncorrelated thermal noise.

The last two topics presented considered different aspects of the performance of the IS-95 uplink and downlink respectively.

Benthin et al. from the University of Hamburg–Harburg, Germany, evaluated a chip time aligned Rake receiver for modulation similar to the IS-95 uplink. The channel model was based on the COST 207 bad urban model with Rayleigh fading. A comparison between coherent maximal ratio combining and non coherent combining of the multipath components was presented. For the latter case, two strategies were adopted for limiting the number of paths selected: either restrict to 5 or threshold at 20% of the largest. Both of these strategies gave similar performance but the difference between performance for the coherent and the non coherent receiver was very significant, corresponding to a capacity ratio of about 2.5:1 at 4% BER.

Finally, Beck et al (University of Ulm, Germany) presented simulation results for modulation similar to the downlink of IS-95. The COST 207 typical urban channel along with measurements in Frankfurt and Darmstadt was used in the evaluation. The motivation of this work was to examine the effects of increasing multipath diversity which, on the one hand increases immunity to multipath fading but, on the other hand, destroys the inherent orthogonality of the Walsh function based signal. The most interesting results are shown in Fig. 6.16:

The "1 User" results indicate the performance without reference to CDMA orthogonality. Here Channel 1 is much better than Channel 2. However, with multiple users, the higher intra–user interference for Channel 1 resulted in performance significantly
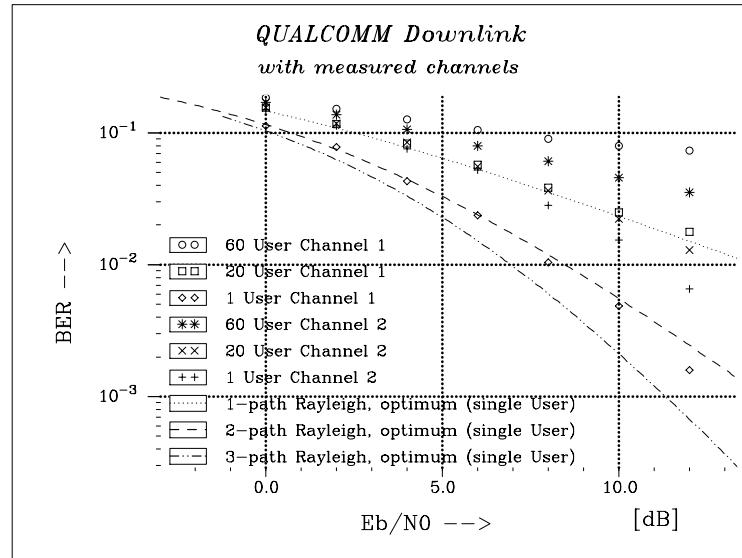
Figure 6.16: Simulation Results for IS-95 Downlink with Channel 1 (Frankfurt measurements) and Channel 2 (Darmstadt measurements)

worse than for Channel 2 under the same conditions.

Power Control

The uplink of a CDMA mobile radio system was shown to be heavily influenced by the near far effect unless power control is applied. Further work, by R. Prasad et al (Delft University of Technology, Delft, Netherlands) explored the influence on capacity of power control imperfections, expressed in terms of numbers of users versus power control error standard deviation. Fig. 6.17 shows the results. It should observed that the protection ratio figure of 7 dB used in the analysis was obtained from [54]. This reference obtained the protection ratio figure in the presence of power control imperfections due to fading. Thus the power control variation specified in Fig. 6.17 would be due to some additional phenomenon.

In evaluating the downlink of such a system, a sharp distinction is made between single and multiple cell systems. It was shown that power control is unnecessary (from the viewpoint of capacity) for a single cell systems since all users receive the interference over the same path as the signal and therefore at the same relative level. However, for the multiple cell case, it was shown that mobiles near the edge of the cell receive significantly more interference from other base stations. By controlling C/I at each of the mobiles a significant improvement in capacity was shown.

Two research groups examined the overall power control strategy and its effect on
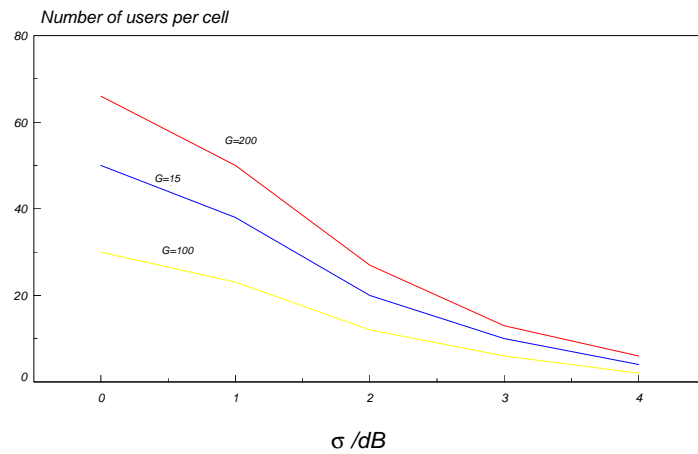
Figure 6.17: Uplink capacity as function of power control imperfection for three values of the processing gain G, outage propability=0.01 and voice activity $a = 0.375$

capacity. Nadal et al (Barcelona, Spain) compared two power control strategies: a simple approach in which the SIR values are equalised within each cell but not from cell to cell and a centralised approach in which the SIR values are equalised over the entire deployment. It was shown that the latter approach led to significantly higher capacities than the former, particularly in the case of a non uniform distribution of mobiles.

At 1% blocking with $\alpha = 4$ (power law) the capacity increase is of the order of 20% in the uniform traffic case. In the specific case of non uniform traffic evaluated, the increase was about 25%. These results were corroborated by G. Falciasecca et al (Universita di Bologna, Italy) who used a similar approach and also showed a capacity increase of around 20%, this time at 5% blocking.

Modulation and Bandwidth Limitation for CDMA Transmission

This subsection considers the issue of modulation and bandwidth limitation for CDMA transmissions and relates to work performed by Aldis & Barton (University of Bradford, UK). The first work reported was a simulation of Butterworth filtered QPSK received using a fully matched correlator (oversampled with filtered correlator sequence). The simulation result was the effective processing gain based on interference consisting of like–modulated users, both synchronised and unsynchronised to the target signal. It was shown, for synchronised interferers that the effective processing gain rose linearly with filter bandwidth up to the point where the (double sided) filter bandwidth was equal to the chip rate (Fig. 6.18).
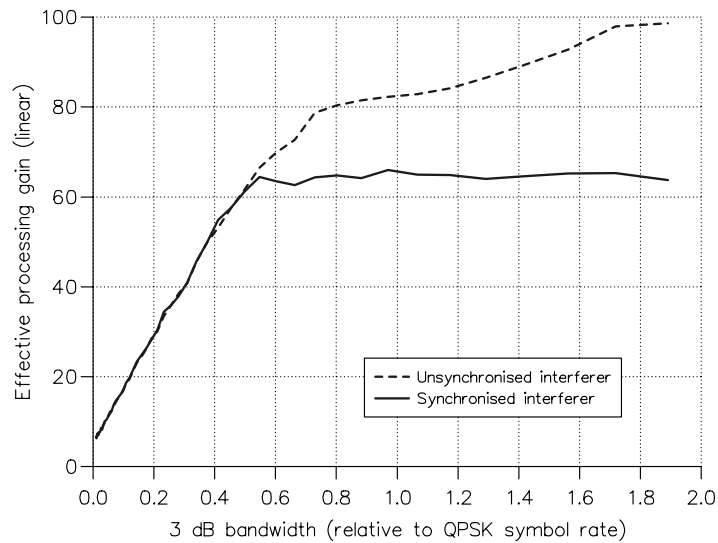
Figure 6.18: Performance of Low Pass Filtered DS–CDMA, 64 chips per bit

If the spreading factor were defined as the ratio of the signal bandwidth (as defined by the filter bandwidth) to the data symbol rate, then we would see that the processing gain is approximately equal to this spreading factor for all filter bandwidths up to the chip rate. Beyond this point, the relative processing gain falls. Thus the optimum bandwidth is equal to the chip rate. For unsynchronised signals, the processing gain continues to rise with increasing filter bandwidth but in spite of this, the relative processing gain falls since the filter bandwidth rises more rapidly than the processing gain.

The second activity examined the use of GMSK for spreading modulation and explored the processing gain as a function of the bandwidth of the pre–modulation Gaussian filter. Again, the interference was like modulated signals rather than AWGN. In this case, two receiver types were evaluated, one (complex) based on the full matched filter, the other (simple) involving multiplication by the same pseudo random bit sequence as that used in the transmit filter at the instants of maximum "eye opening". The results are shown in Fig. 6.19. The curves are plotted against the time–bandwidth product of the Gaussian filter.

When the time bandwidth product is small, the simple receiver is inferior to the complex receiver as expected because of the high ISI under these conditions. Synchronous and asynchronous interference behaves similarly. At high bandwidths unsynchronised interferers lead to significantly larger processing gains. Surprisingly, the simple receiver significantly outperforms the complex receiver under this condition.
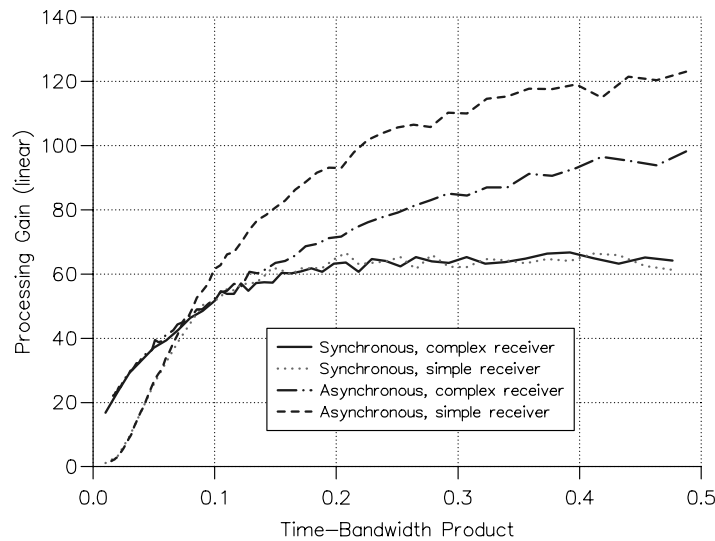
Figure 6.19: Effective Processing Gain of DS–CDMA systems using GMSK

The overall conclusion is that GMSK leads to slightly poorer performance than filtered QPSK when the actual occupied bandwidths are used to define the spreading factors although the difference will depend upon the definition of occupied bandwidth.

Code Set Selection for Synchronous CDMA (S-CDMA)

This section covers work done by Tanik et al. (Electric. Electron. Eng. Dept, METU, Ankara, Turkey) to find optimum code sets for CDMA system in which all spreading sequences are synchronised to a fraction of a chip (intra cell and inter cell, both uplink and downlink). This is referred to as Synchronous CDMA (S–CDMA).

The system investigated had N (N=31 or 32) mobile users per cell, a spreading ratio of N_p $(N_p = N)$ and a code reuse pattern of 4. The base stations and the mobile units transmitted TDD bursts synchronously. Since the system was designed mainly for indoor use the cellular structure employs picocells and thus the communication medium could be a flat fading Rayleigh channel. Consequently, time delays due to propagation remained in one chip interval. Power control was employed in the uplink path within a cell, so all signals from the users of the same cell were received with equal power by the base station. However, the signal coming from any mobile of the neighbouring cells experienced a path loss factor denoted by α, a random variable depending on the communication medium and the relative position of the mobile with respect to the base station of concern. In the analytical study, an average α was used for all mobile users of neighbouring cells. Communication was maintained via two orthogonal chan-

nels (inphase and quadrature) and convolutional FEC of rate 1/2 was used to provide a BER of 10^{-3} which is sufficient for reliable communications. Spreading was performed on a single coded bit in each channel. For the uplink, the total multiple access interference affecting any user is directly proportional to the mutual cross–correlations between that user and the other users of the system. Thus spreading codes with low correlation parameters are required. Conventionally, maximal–length shift register sequences (m–sequences) have been used because of their appealing correlation properties. However, m–sequences are still above the theoretical Welch bound. The study aimed to find spreading code sequences with better performance than m–sequences.

The problem of designing a low correlation codebook which contains $4N$ bipolar sequences of length N was formulated as a constrained optimisation problem. The codewords were arranged as rows of a $4N \times N$ codebook matrix. The optimisation criteria was to minimise the maximum of the total interference encountered by all the users of the system.

Two stochastic global optimisation techniques were applied: Genetic Algorithms and Simulated Annealing, but the results obtained are not promising. This was believed to be because of the high dimensionality and the discrete nature of the problem. Given this, more computing power would be required.

The additional problem of distributing a given code set among cells was also addressed. When the code set of concern is the set of m–sequences, it was proved that the optimum distribution is the conventional one where all phases of an m–sequence are assigned to a cell. When the code is the large class of Gold Sequences, the problem of selecting codes must also be solved together with the problem of distributing them. The exhaustive solution of this combined problem requires heavy computation. Therefore, another Genetic Algorithm was implemented to solve it and an improvement over m–sequences was obtained.

Finally, an iterative search technique, which performed small perturbations on the existing codebook such as swap/toggle two bits or set to ± 1, was applied. The initial codebook was obtained by placing the 32×32 perfectly orthogonal Hadamard set in all the cells. It was observed that the performance criteria became considerably worse when the slightest perturbation was made on the Hadamard codebook. Furthermore, the Hademard codebook was found to have slightly better performance than the m–sequences. Although it would not be practical to use the Hadamard set in all the cells of the system, it could be effectively used if the codes of the users were dynamically assigned according to their relative positions. This problem of dynamically assigning codes is a new topic for further study.

System Capacity

This subsection covers overall system capacity evaluations. Hulbert et al (Roke Manor Research, Romsey, UK) performed an overall evaluation of CDMA based on the IS-95 Uplink. This evaluation covered simulation of re–use efficiency, and voice activity detection taking account of statistical fluctuations and using the 99 percentile in both

cases, leading to very conservative figures. In this evaluation, an absolute worst case re–use efficiency of 0.48 was derived. This was based on log normal shadowing at 8 dB standard deviation and a graded range law, becoming fourth law beyond the cell boundary. The voice activity factor of the IS-95 variable bit rate coder operation, derived using a Markov model, was 63% at the 99 percentile (the mean figure was 45%). The uplink E_b/N_0 requirement for 10^{-3} BER was derived by simulation as 5.1 and 6.5 dB for 10 and 30 mph respectively. A comparison with half rate GSM indicated higher spectral efficiency for CDMA when both systems used sectored antennas.

An Italian collaboration among the University of Bologona, Fondazione U. Bordoni and CSELT performed a detailed theoretical study of the effect of propagation characteristics on spectral efficiency. As propagation model a path loss proportional to $r^{\gamma} \cdot 10^{\xi/10}$ was assumed, where r is the transmitter–to–receiver distance, γ is the propagation factor and ξ is a random, normally distributed variable, simulating the shadow fading and characterised by zero mean and standard deviation σ (in dB). Ordinarily, analytic evaluations of CDMA with shadowing are precluded because of the need, on occasions, to alter the mobile affiliation according to the shadow depth. This work analytically generated an upper bound on re–use efficiency by limiting, for every interferer, the ratio of shadow depth to the nearest cell to the shadow depth to the cell of interest whenever the cell of interest would otherwise become the preferred cell for affiliation. Fig. 6.20 illustrates the performance results for a particular case. It shows, for example that, with 8 dB shadow standard deviation, the capacity increases by about 57% when the range law changes from 3 to 5.
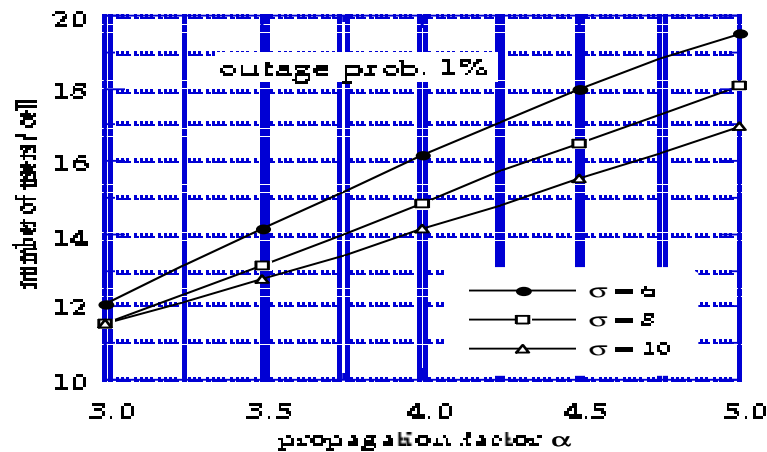

Figure 6.20: Number of Users against propagation factor, α with outage probability 1% and various propagation standard deviation factors, σ

Gaiani & Palestini (CSELT, Torino, Italy) have evaluated system capacity in a multicell system with at least two tiers of interfering cells around the reference one and a uniform distribution of static users within the overall area. The same propagation model as described above was used. The most important differences between the two links are related to the power control methodology: In the uplink a sort of ideal open loop (based on the path loss estimation on the base–to–mobile link) was applied, while in the downlink a C/I driven control was adopted.

Fig. 6.21 shows that the application of a C/I–driven power control improves the C/I ratio by about 4 dB in the downlink, at an outage probability of 10%, with respect to the case of no power control. The performance is similar, although slightly lower, to that obtained for the uplink using ideal open loop control. The performance difference in the two directions was due to the fact that, in the simulated model, the external interference was slightly greater than in the uplink in the average of the cases. However, it was verified that, at an outage probability of 1%, the uplink is more critical.

In both links the performance is better for an urban area (here simulated through a propagation factor $\gamma=5$ and a standard deviation of the shadowing $\sigma=10$ dB) than for a rural area ($\gamma=3$, $\sigma=6$ dB) by a factor equal to 54% in terms of capacity, (see Fig. 6.22) if E_b/N_0 ratio equal to 7 dB and a processing gain $G = 128$ are assumed (for instance 16, 17 users/site in urban area and 10, 11 users/site in rural area).
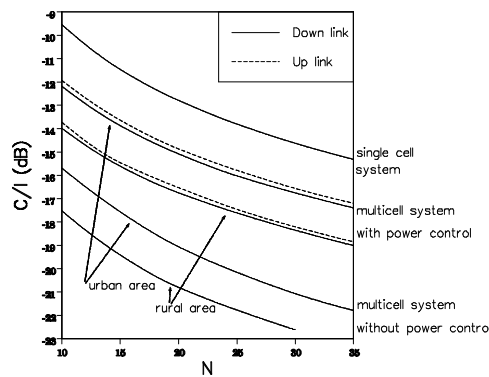

Figure 6.21: C/I ratio vs the number of user per cell computed (for both links) at an outage probability of 10%, for both a single and a multicell system with the base stations equipped with omnidirectional antennas, in a rural area and in an urban area, when power control is applied and when it is not applied.
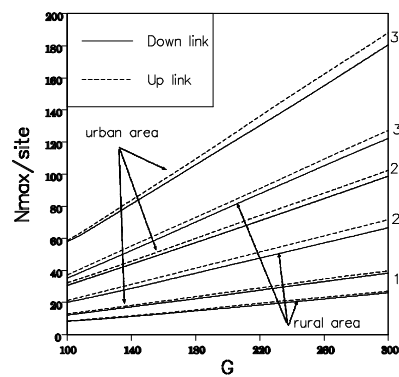
Figure 6.22: Maximum number of users per site vs the processing gain computed (for both links) for a multicell system equipped with omnidirectional antennas (curves 1), 120–degree (curves 2) and 60 degree (curves 3) sector antennas, in a rural area and in an urban area, when power control is applied
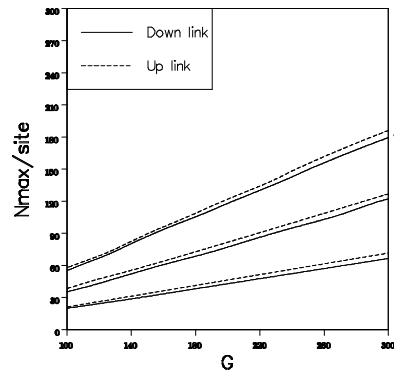
Figure 6.23: Maximum number of users per site vs the processing gain computed (for both links) for a multicell system equipped with 120-degree sector antennas in a rural area with power control and without application of VAD (curves 1), and with VAD under the hypothesis that the transmission rate is equal to 0.29 times the normal rate (curves 2) or equal to 0 (curves 3) if there is no speech.

Figure 6.24: Maximum number of users per site vs the processing gain computed (for both links) for a multicell system equipped with 120–degree sector antennas in an urban area with power control and without application of VAD (curves 1), and with VAD under the hypothesis that the transmission rate is equal to 0.29 times the normal rate (curves 2) or equal to 0 (curves 3) if there is no speech.
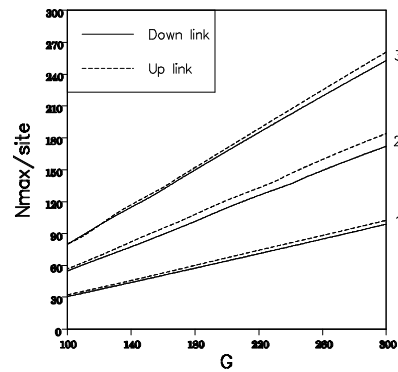
If the base stations are equipped with directional antennas the capacity gain factor due to cell sectorization is about 2.6 in the case of 120–degree sectorization and about 4.6 in the case of 60–degree sector antennas. These values have been found for both links and for both urban and rural area.

The application of VAD (voice activity detection) was shown to cause an improvement of the capacity (in both directions, for both rural and urban areas) of about 1.8, if, in the case of no speech, the signal is assumed to be transmitted at a reduced rate equal to 0.29 times the normal rate. The results are shown in Fig. 6.23 and 6.24 for rural and urban areas respectively.

The VAD gain becomes about 2.6 if no signal is transmitted when there is no speech. Therefore it was concluded that a DS–CDMA system could increase its capacity by a factor roughly equal to 4.5 if, for instance, three–cell sectorization and VAD are applied. Under these conditions, the number of users/site was equal to 50 for a rural area and 75 for an urban area. The above described gains were found to be independent of the processing gain, at least in the range up to 300.

A simulation of hot spot conditions was performed, for which the result were found to be similar for both directions. For example, with a fixed number of users in the whole simulated area, if the number of users in the hot spot doubled, while maintain-

ing a uniform distribution of terminals in the other cells, the degradation of C/I ratio evaluated in the hot spot cell at an outage probability of 10% was about 1.5 dB in a rural area and about 2 dB in an urban area, as a consequence of the increased internal interference which has a greater effect than the reduction of the external contributions.

Acquisition of DS Code Phase

Before any of the DS–CDMA systems described earlier in this section can operate, a local version of the spreading code clock in the receiver must be synchronised to the received code. Synchronisation is achieved by correlating all possible phases of the local code against the received signal until a particular phase leads to a correlation output conclusively indicating correct de–spreading of the signal. The different phases may be handled serially, in parallel or any combination of the two. Moreover, a number of successive correlations on the same search phase (dwells) may be performed, to advantage, as part of the search strategy.

A simple serial synchroniser would despread the signal once for each code phase in turn, comparing the resultant energy against a threshold. This threshold would need to be set high enough almost to eliminate false alarms (to avoid considerable increase of synchronisation time due to false synchronisation). This high threshold would in turn lead to a low probability of detection, requiring many search cycles to detect the signal. In a multiple dwell strategy, a low threshold is set for the initial dwell on each code phase (resulting in significant initial detection rates). Various strategies of subsequent dwells are then used to determine whether the current phase is the correct one.

Professor Simsa et al (Inst of Radio Eng & Electronics, Academy of Sciences of the Czech Republic, Praha) examined multiple dwell serial search strategies for signals with low signal–to–noise ratio (typically -6 dB) following de-spreading. Operating at these low signal–to–noise ratios permits short integration periods, thereby allowing synchronisation in the presence of significant frequency uncertainty.

Many different multiple dwell algorithms could be considered. Two of those evaluated were the "up–down counter" (UDC) and the "two step rejection" (TSR) algorithms. Both involved an initial correlation followed by a sequence of I verification correlations. In the case of the UDC, a failure at the i–th correlation leads to a repeat at the $(i-1)$–th stage (except for the 1st stage which leads to an immediate reject). In the case of TSR, a failure at any stage is followed by a second observation. Failure here leads to immediate rejection. Success resets the verification back to the beginning.

Some of the results generated by a detailed theoretical analysis of the AWGN case are illustrated in Fig. 6.25 and 6.26. Where: T_a is the acquisition time in bits; L is the code length; q is number of search cells ($\leq$ twice code length for 1/2 chip steps); ϑ is the penalty (in bits) of false detection; δ_1 and δ_2 are the threshold during initial and verification correlations respectively; I is the number of verification steps; M_1 and M_2 are the initial and verification correlation times in bits respectively. δ_2 is optimised individually for each value of I. It is seen that the UCD performs significantly better
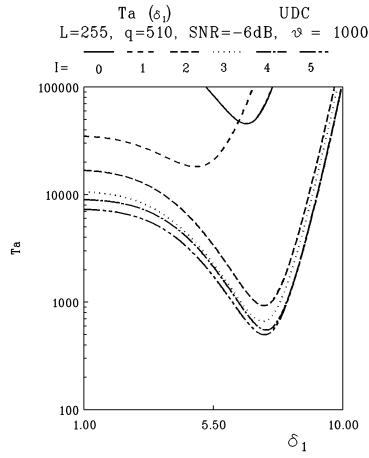
Ta (δ_1) UDC

L=255, q=510, SNR=−6dB, ϑ = 1000

I=   0   1   2   3   4   5

Figure 6.25: T_a versus δ_1 for UDC with $M_1 = 1, M_2 = 5$

Ta (δ_1) TSR

L=255, q=510, SNR=−6dB, ϑ = 1000
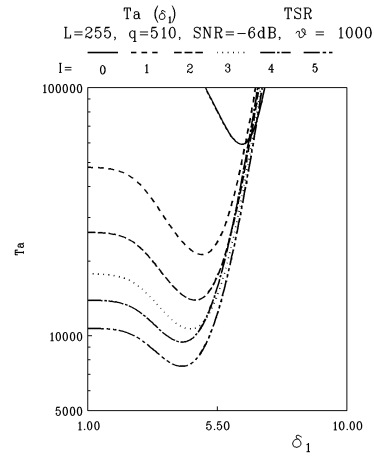
I=   0   1   2   3   4   5

Figure 6.26: T_a versus δ_1 for TSR with $M_1 = 1, M_2 = 5$

than the TSR.

Yuan Wu at CNET, also analysed serial and parallel search strategies with matched filter detection. Fig. 6.27 illustrates the correlation signal detection part of the system. The input signals are digital samples at complex baseband. Like most acquisition systems, the system (examined with serial or parallel search strategy) works in either search mode (S_{mode}) or verification mode (V_{mode}) It starts in the S_{mode} and may go into the V_{mode}. In S_{mode}, each sample of the correlation signal Cs represents one of the possible cells (PN-sequence alignments). In V_{mode}, all the samples of Cs correspond to one specific cell. The PN-sequence generating device gives the local PN-sequence and ensures that the switching of the operation modes is done as rapidly as possible.
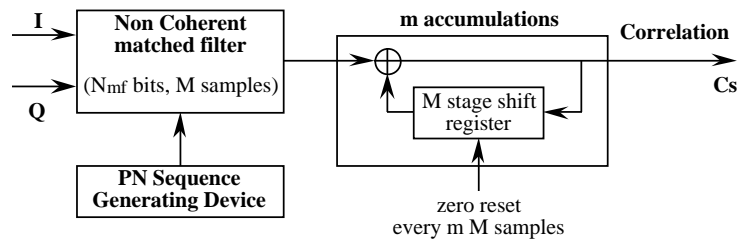
Figure 6.27: The correlation signal detection scheme

For the serial search strategy, the S_{mode} consists in the comparison of the samples of *Cs* with a threshold β until the system finds a sample greater than β, then at the corresponding cell, the V_{mode} tests *A* independent samples: if there are at least *B* samples greater than β, the acquisition is declared, if not, the system goes back into S_{mode}. The parallel search strategy works as the serial except in the S_{mode} where it searches the maximum *Cs* sample among all the samples of the possible cells and switches the system in V_{mode} for the corresponding cell.

The system performance, given by the mean acquisition time, T_a, would normally be calculated using the probability density function (pdf) of the correlation signal *Cs*. Because determination of the exact pdf expression would take considerable computer time, a simplified pdf expression was generated, based on the following model: the auto-correlation noise was artificially divided into two zero mean, independent and equal variance noise components, one in-phase with the auto-correlation signal; the other in quadrature. The sum of their variances was made equal to that of the auto-correlation noise. The numerical results showed that the approximate values of T_a obtained by use of the simplified pdf expression was very close to the exact value, for both search strategies.

The Nyquist pulse shape was found to be better than the rectangular pulse shape because it gives a small sensitivity to the offset of the local chip clock when the number of samples per chip is more than one. Two samples per chip were found to be sufficient to give acceptable degradation in T_a.

The two search strategies were compared in different situations. In general, it was concluded that it is better to use the parallel strategy when the N_{mf} is large and *m* small. In the case of N_{mf} small and *m* large, the serial strategy appeared more interesting. When the PN-sequence length is small, the parallel strategy is better; but when it is larger, the serial strategy becomes the better. The influence of a non optimum threshold was also studied and the parallel strategy appeared more robust than the serial strategy.

Tracking of DS Code Phase

In a CDMA system a DLL (Delay Locked Loop) can be used to keep fine tracking of the received code phase. In a narrow-band system, where the receiver can not resolve the different propagation paths, deep signal fadings are likely to happen due to multipath. As the DLL parameters (closed loop gain, noise bandwidth, etc) depend on the received signal power, its performance can be severely degraded with respect to the static channel situation [55]. In this situation the DLL will frequently lose lock due to noise. In order to measure the DLL performance, one key parameter is the mean time between two consecutives losts of lock (MTLL). Assuming a wide-band transmission system, the receiver may have enough bandwidth to resolve more than one propagation path. In this case we can make use of the fact that the signals arriving from different paths have been independently faded and use a modified DLL scheme that, like a diversity system, takes advantadge of multipath. Fig. 6.28 is a block diagram of the proposed DLL assuming that we can resolve a second propagation path with a delay
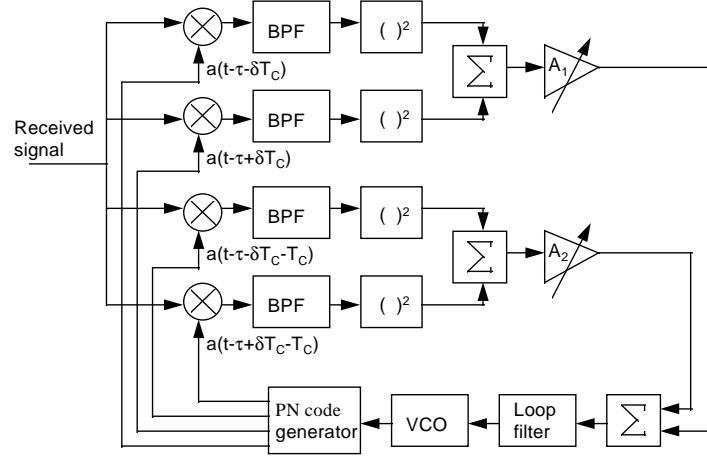
Figure 6.28: Block diagram of the proposed DLL

of T_C seconds (one chip interval) with respect to the first one. In Fig. 6.28 we can see how the error signal of the loop is obtained by adding the weighted contributions of two independent delay detectors working with local PN code sequences that are phase shifted by T_C seconds. As shown in [55], the weights A_1 and A_2 should be proportional to the signal to noise ratio in each path.

In order to assess the performance of the proposed scheme, computer simulations have been carried out. The results show a remarkable improvement with respect to the conventional (single delay detector) DLL. Tab. 6.7 shows the logarithm of the obtained MTLL normalized to B, the bandwidth of the data signal. The product MTLL $\cdot B$ can be interpreted as the MTLL expressed in bit periods. In Tab. 6.7 σ is the doppler spread of the channel and γ_2 is the mean signal to noise ratio in the second path.

γ_2(dB)	$\sigma/B = 0.001$ $\log(\text{MTTL} \cdot B)$	$\sigma/B = 0.01$ $\log(\text{MTTL} \cdot B)$
-15	4.55	4.48
-10	4.66	4.58
-5	5.27	5.34
0	6.3	6.45
5	7.33	7.5

Table 6.7: Mean time between two consecutives losts of lock (MTLL) under different channel conditions using the DLL shown in Fig. 6.28

The signal to noise ratio in the first path is constant and equal to 5 dB. The situation $\gamma_2 = -15$ dB is almost equivalent to a narrow band system, since the weight of the second path is very small. It can be verified that two paths with the same signal to noise ratio (5 dB) give a MTLL = 48 minutes with 100 Hz of doppler spread and $B = 104$ Hz.

A different approach to the above DLL based schemes has been also considered to improve the performance of a tracking scheme of DS code phase. In particular, these schemes are optimum for a AWGN channel but not for operation in frequency-selective fading channels, like those encountered in mobile communications.

A first attempt to introduce specific synchronizers for operation in those environments was presented in [56], where an Extended Kalman Filter structure was proposed to jointly estimate the PN code delay in tracking and the channel impulse response. Nevertheless, this approach fails in the presence of high-interference environments, usual in mobile communication systems. Pilar Díaz and Ramón Agustí from UPC proposed and analysed a scheme based on the EKF approach, but conveniently modified in order to improve its performance in terms of MTLL (Mean Time to Lose Lock) and the mean root square estimation (jitter) error when operating under realistic conditions (i.e., signal-to-interference input ratios from -20 dB to 0 dB). The performance of this scheme was assessed by means of computer simulations for band-limited Nyquist-filtering receivers (see [57]).

In [56] it is shown that the EKF is capable of estimating the channel delay in the tracking phase from the received samples and maintaining synchronization between the received code and the local code. However, this delay estimator only works whith large signal-to-interfering ratios at the receiver input. Since this is not the usual condition in a CDMA cellular system, some signal processing before estimation is required. For the sake of improving this signal-to-interfering power ratio, the proposed delay estimator consists of two blocks: a first block known as "pre-filter", responsible for processing the received signal and improving the signal-to-interfering power ratio, and a second block, which is the EKF, now capable of estimating the channel delay in a CDMA environment.

As an example of the estimator performance, Fig. 6.29 shows the normalised jitter for rectangular and Nyquist pulses. The values obtained show that the rms jitter is lower than the 10% of the chip interval, T_c, even for $SIR = -20$ dB.

6.4.2 FH-CDMA

Conventionally, CDMA systems use direct sequence spread spectrum (DSSS). However, frequency hopping (FH) is equally applicable. Slow FH has the advantage of allowing orthogonal transmission for both the downlink and the uplink, whilst preserving the benefits of multipath and interferer diversity. A combination of TDMA with slow frequency hopping is covered in Section 6.6. It is also possible to use slow frequency hopping without a TDMA element and re–use the same contiguous frequency band in all cells in the same way as for DS–CDMA.
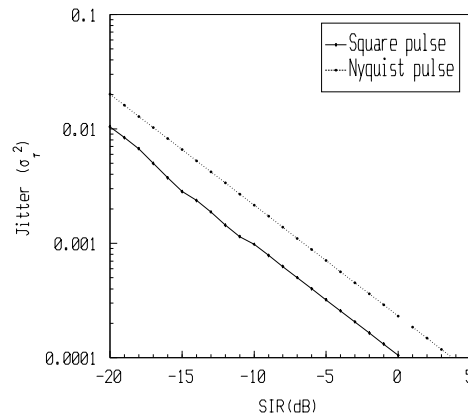
Figure 6.29: Normalised jitter for rectangular and Nyquist pulses in terms of *SIR*

Livneh, Ritz, Silbershatz (Rafael) & Meidan (Motorola) evaluated a slow frequency hopping solution with the following parameters: 500 hops per second over 12.5 MHz; intra cell hopping orthogonal - with accurate uplink sychronisation; intercell - minimal cross correlation; interleaving over 20 hops (for multipath and interferer diversity); frequency spacing of 16 kHz; modulation $\pi/4$–QPSK; data rate 12 kbit/s overall with 8 kbit/s dedicated to coded voice; half rate convolutional coding – constraint length 9; voice activity detection and modest performance power control applied.
Simulation results projected 2295 active users per 3 sectored cell, corresponding to a capacity 35 times greater than AMPS. The one way interleaver delay was 40 ms.

6.4.3   Hybrid DS/SFH CDMA

This subsection presents work performed by R. Prasad (Delft University of Technology, Delft, Netherlands) on throughput and delay analysis of a packet–switched CDMA network. The performance of the network was investigated with three CDMA techniques, viz. Direct Sequence (DS), Slow Frequency Hopping (SFH) and hybrid DS/SFH, where both an analytical channel model and measured channel characteristics were used. Furthermore the effects of modulation techniques, selection diversity and Forward Error Correction (FEC) codes on the performance were evaluated.

Network description

The network, which consisted of C users all communicating with the same basestation, had the following characteristics: i) Data transmitted in packets of N_p bits; ii) Slotted; iii) Time slot equal to packet duration; iv) Positive acknowledgement scheme. In order to be able to give some close expressions for the throughput, the following five

assumptions were made: i) all users identical from a statistical point of view, the same holding for the transceivers at the base station, ii) the averaged received power at the base station common to all users, iii) acknowledgements almost cost free from a capacity point of view, fully reliable and instantaneous, iv) channel memoryless and v) system in a stable state.

Analytical and measured channel models

In case of the analytical channel the following assumptions were made concerning the channel parameters: i) Rician distributed path gains, β_{kl} ; ii) delays, τ_{kl}, uniformly distributed random variables over [0,T]; iii) phases, γ_{kl}, uniformly distributed over [0,2π]. The channel was assumed to be slow fading, leading to random variables which did not change considerably for the duration of one packet. The Rice parameter R is defined as the ratio of the power associated with the specular signal component $A^2/2$ and the power associated with the scattered components σ [53, 58]. This parameter incorporates the radio characteristics of the environment. In the measured pico cellular channel model the true measured values of the path gains were used for the calculations [59].

Throughput and delay analysis

The throughput S is defined here as the expected number of successfully received packets per time slot, given by [58]:

$$S = \sum_{k=1}^{C} k \cdot p_k \cdot P_k^t(k)$$

where p_k is the probability density function of the composite arrivals in a given time slot. For identical, independent and a finite number of users, this PDF was shown to be a binomial distribution given by:

$$p_k = \binom{C}{k} \cdot \left(\frac{G}{C}\right)^k \cdot \left(1 - \frac{G}{C}\right)^{C-k}$$

where the offered traffic G is defined as the average number of transmissions (new plus retransmitted packets) per time slot by C users. P is the packet success probability, which incorporates the effects of fading, modulation, FEC coding and diversity. The average normalised delay D of the system is defined as the average number of time slots between the generation and the successful reception of a packet. According to [4] the normalised delay is given by:

$$D = 1.5 + \left(\frac{G}{S} - 1\right) \cdot \left(\lfloor \delta + 1 \rfloor + 1\right)$$

where $\left(G/S - 1\right)$ represents the average number of retransmissions needed for a packet to be received successfully and δ denotes the mean of the retransmission delay. The

round trip propagation delay can be neglected in a pico cellular environment. Tab. 6.8 presents the throughput S normalised on the offered traffic G for Q–, B– and DPSK modulation with the order of selection diversity M as a parameter, where L is the number of resolvable paths and N_d and N_b are the spreading code lengths for D– and BPSK respectively and q is the number of hopping frequencies. QPSK yields relatively the largest throughput and DPSK relatively the poorest. Selection diversity enhances the performance in comparison with nondiversity ($M = 1$).

Order of diversity	S for QPSK	S for BPSK	S for DPSK
$M = 1$	51,8 %	48,1 %	32,9 %
$M = 2$	63,8 %	60,0 %	44,1 %
$M = 3$	69,0 %	65,9 %	50,0 %

Table 6.8: Comparison of the maximum throughput S normalised on the offered traffic G of the hybrid DS/SFH system with Q–, B– and D–PSK for $M = 1$, 2 and 3. $N_q = 255$; $N_b = N_d = 127$; $q = 10$; $L = 3$ at fixed bandwidth.

In Fig. 6.30 the throughput of hybrid DS/SFH is compared with the throughput of pure DS and SFH for B– and Q–PSK modulation using FEC coding an the analytical channel model and for a fixed bandwidth. The comparison is done according to [60] where $N_q = 2N_b$.
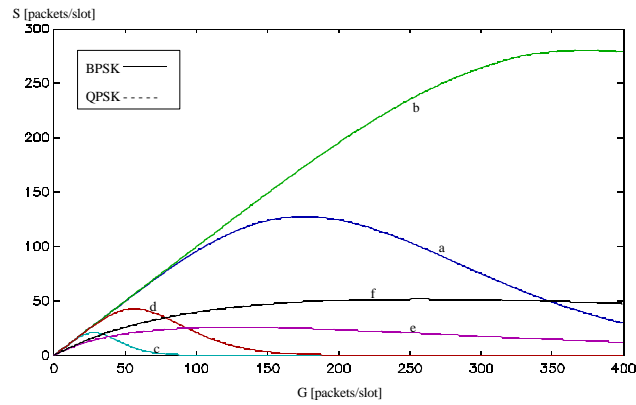

Figure 6.30: Hybrid DS/SFH, DS and SFH with (23,12) Golay coding. a) hybrid: $L = 3$, $q = 10$, $N = 63$ b) hybrid: $L = 3$, $q = 10$, $N = 127$ c) DS: $L = 21$, $N = 630$ d) DS: $L = 21$, $N = 1270$ e) SFH: $q = 630$, $L = 1$ f) SFH: $q = 1270$, $L = 1$

Dn [slots]

MPD, Rb=250 kbit/s, N=127

K= 400
Bandwidth= 200 MHz
SNR= 20 dB
q= 6

IID, Rb=250 kbit/s, N=127

IID, Rb=125 kbit/s, N=255

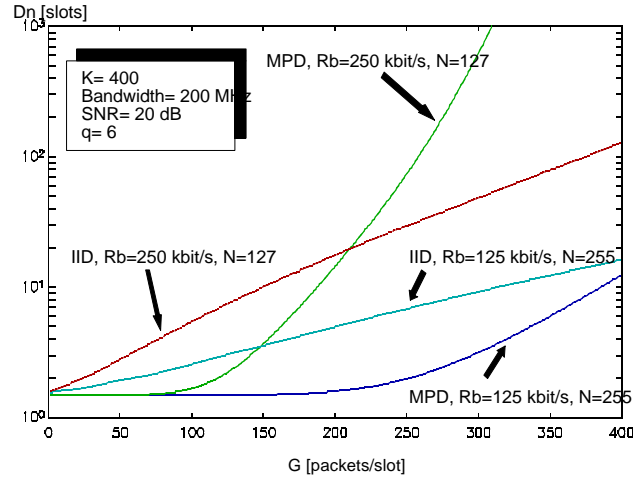MPD, Rb=125 kbit/s, N=255

G [packets/slot]

Figure 6.31: Delay performance of hybrid DS/SFH with BPSK modulation, using a measured and analytical channel model

It is seen that the hybrid DS/SFH technique has the highest throughput. Moreover, the maximum throughput values for both SFH and DS are almost equal, although the throughput for SFH doesn't vary much over the large range of G. In Fig. 6.31 the delay of hybrid DS/SFH, using the measured channel model has been compared with the performance using the analytical model. The rms delay spread is taken equal to 10 ns.

It is seen that the delay obtained using the MPD channel model is lower than in case of the analytical IID channel model. For higher bit rates the delay is higher than for lower bit rates.

6.5   CDMA with multi-user detection

P.W. Baier, University of Kaiserslautern, Germany (6.5.1)
A. Klein, University of Kaiserslautern, Germany (6.5.1)
D. Dahlhaus, Swiss Federal Inst. of Technology, Switzerland (6.5.2)
A. Radović, Swiss Federal Inst. of Technology, Switzerland (6.5.2)
G. Romano, CSELT, Italy (6.5.3)
T. Frey, University of Ulm, Germany (6.5.3)

6.5.1   Joint detection CDMA

In CDMA mobile radio systems, a number K of independent users are simultaneously active in the same frequency band, only discernible by different user–specific spreading codes. Each data symbol of the data symbol sequence $d^{(k)}$ transmitted by user k is multiplied by the user–specific spreading code. The resulting signal of user k is transmitted over the time–variant multipath mobile radio channel. In the uplink, the mobile radio channels of all K users are in general different. At the receiver of the base station, the superposition of the contributions of all K users appears. At the receiver, transmission over the time–variant multipath mobile radio channels results in both intersymbol interference (ISI) between the data symbols of one and the same user and multiple access interference (MAI) between data symbols of different users. MAI is also termed inter–user interference (IUI). The superposition signal is also disturbed by a sequence n representing intercell interference and thermal noise. The received sequence e containing samples at the chip rate has to be processed at the receiver by a data detection algorithm to determine estimates $\hat{d}^{(k)}$ of the data symbol sequences $d^{(k)}$, $k=1 \ldots K$, of all K users.

The conventional suboptimum single–user receiver is implemented as a bank of K matched filters or K RAKE receivers, which consider each user as if it were the only one present. This is inefficient since MAI is treated as noise. In mobile radio systems using single–user receivers, measures as accurate power control combating fast fading, voice activity monitoring, antenna sectorisation and soft handover are necessary to obtain an acceptable performance. These measures as well as synchronisation at the chip level can be avoided when applying multi–user receivers, which exploit a–priori–knowledge about both ISI and MAI. In addition, however, when applying multi–user receivers, the above–mentioned measures can be beneficially employed. The optimum multi–user receiver is too complex to be implemented in third generation mobile radio systems. Therefore, suboptimum multi–user receiver techniques were proposed and investigated in COST 231. Concerning JD techniques, the four equalisers

- zero forcing block linear equaliser (ZF–BLE),
- minimum mean square error block linear equaliser (MMSE–BLE),
- zero forcing block decision feedback equaliser (ZF–BDFE),
- minimum mean square error block decision feedback equaliser (MMSE–BDFE)

were developed and extensively investigated. These four equalisers, which perform JD, are designed for

- multipath channels and
- burst transmission.

The transmission can be described mathematically by the matrix–vector–expression

$$e = A\,d + n \tag{6.1}$$

with the received vector e, which is a function of the combined data vector d, the system matrix A, and the interference and noise vector n. The combined data vector d contains all transmitted data symbol sequences $d^{(k)}$, $k=1...K$, of all K users. The system matrix A is determined by the spreading codes of all K users and the mobile radio channel impulse responses of all K users. The mathematical description (6.1) is valid for the uplink as well as for the downlink, and for the case of one receiver antenna as well as for the case of more than one receiver antenna. The derivation of (6.1) and the exact definitions of e, A, d and n can be found in [61, 62] for the case of one receiver antenna and in [63] for the case of more than one receiver antenna.

(6.1) represents a system of linear equations. At the receiver, this system, which is time–variant, has to be solved in order to determine an estimate $\hat{d}$ of d. For solving this system of linear equations, it is assumed that, besides the received vector e, the spreading codes of all K users and the mobile radio channel impulse responses of all K users and thus the system matrix A are known at the receiver. When using training sequences, the K mobile radio channel impulse responses can be estimated at the receiver by an algorithm for joint channel estimation which was developed within COST 231. A detailed description of this algorithm can be found in [64]. The system of linear equations (6.1) can be solved according to the criteria zero forcing (ZF) or minimum mean square error (MMSE), which lead to two different approaches for jointly determining an estimate $\hat{d}$ of d. Assuming additive white Gaussian noise of variance σ^2 and uncorrelated data, the ZF–BLE yields the estimate

$$\hat{d}_{\mathrm{ZF}} = \left(A^{*\mathrm{T}}A \right)^{-1} A^{*\mathrm{T}} e \tag{6.2}$$

and the MMSE–BLE gives the estimate

$$\hat{d}_{\mathrm{MMSE}} = \left(A^{*\mathrm{T}}A + \sigma^2 \mathbf{I} \right)^{-1} A^{*\mathrm{T}} e. \tag{6.3}$$

The symbol $(\cdot)^{*\mathrm{T}}$ denotes complex conjugation and transposition and $\mathbf{I}$ is the identity matrix. Equations (6.2) and (6.3) have the same structure. In the case of the MMSE–BLE, the variance σ^2 of the noise is taken into account, which requires that σ^2 is estimated at the receiver. The ZF–BLE for JD leading to (6.2) is a generalization of the single–user ZF equaliser presented in section 6.2. Also in the case of more than one receiver antenna and coherent receiver antenna diversity (CRAD), (6.2) and (6.3) remain valid, as is explained in [63]. Instead of the inversion of the matrices

$(A^{*\mathrm{T}}A)$ and $(A^{*\mathrm{T}}A+\sigma^2\mathbf{I})$ in (6.2) and (6.3), respectively, Cholesky decomposition of these matrices can be applied, which considerably reduces computational complexity. Furthermore, when applying Cholesky decomposition, decision feedback (DF) can be introduced to improve performance without increasing the computational complexity. Introducing DF in (6.2) and (6.3) leads to the ZF–BDFE or the MMSE–BDFE, respectively. To avoid the impairing effect of error propagation when using DF, a method termed channel sorting has been proposed. Details on the applications of Cholesky decomposition, DF including channel sorting and the extension of the equalisers to the case of non–white noise are given in [65] and [63] for the cases of one or more receiver antennas, respectively.

Concerning the computational complexity of the ZF–BLE, MMSE–BLE, ZF–BDFE and MMSE–BDFE for JD, the most important results are:

- All four equalisers require essentially the same computational complexity.
- The computational complexity required is independent of the size of the data symbol alphabet.

The computational complexity required for JD is larger than that required by conventional suboptimum single–user detectors. However, considering the potential of modern microelectronics, the computational complexity required for JD is feasible already today. Especially in systems as proposed in section 7.4, which include a TDMA component leading to a reduction of the number K of simultaneously active users, the computational complexity required for JD seems to be affordable.

The ZF–BLE, MMSE–BLE, ZF–BDFE and MMSE–BDFE have been applied to the JD–CDMA system proposal described in section 7.4. The performance in terms of simulated bit error rate (BER) P_b versus signal–to–noise ratio E_b/N_0 per bit of the ZF–BLE, MMSE–BLE, ZF–BDFE and MMSE–BDFE for one and for two antenna receivers in the uplink is given in Fig. 6.32. Convolutional forward error correction coding (FEC) with rate 1/2 and constraint length 5 is considered. The system parameters used in the simulations are given in section 7.4. The Rayleigh fading multipath mobile radio channels have been modelled according to the COST 207 model bad urban (BU) area channel with a mobile speed of 30 km/h. 8 mobile stations are assumed to be active simultaneously. To obtain the results in Fig. 6.32, channels have been estimated according to [64], so that the effect of imperfect channel estimation is included. More details about the simulations and simulation results can be found for the cases without FEC in [66] and with FEC in [67]. Details about the achievable cellular spectrum efficiency can be found in [68]. The most important results are:

- The two equalisers ZF–BDFE and MMSE–BDFE with DF show a better performance than the two equalisers ZF–BLE and MMSE–BLE without DF.
- The two MMSE equalisers MMSE–BLE and MMSE–BDFE perform slightly better than the two ZF equalisers ZF–BLE and ZF–BDFE, respectively.
- Coherent receiver antenna diversity with two receiver antennas allows E_b/N_0 to be reduced by about 6 dB to 11 dB depending on the type of terrain as compared

with the case of one receiver antenna. 3 dB of this improvement is due to an
energy gain, the additional improvement is due to diversity.

- When applying coherent receiver antenna diversity with two receiver antennas,
  the performance difference of the four equalisers is smaller than in the case of
  one receiver antenna.

- When applying FEC, the performance difference of the four equalisers is smaller
  than in the case where no FEC is applied.

- The achievable cellular spectrum efficiency is of the order of 0.2 bit/(s·Hz) per
  base station in the uplink [68] and 0.39 bit/(s·Hz) per base station in the down-
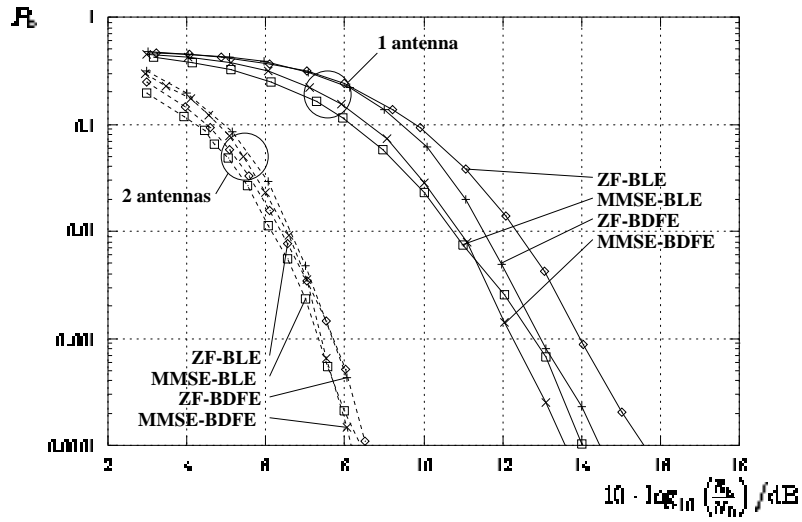 link [69].

Figure 6.32: BER performance of the ZF–BLE, MMSE–BLE, ZF–BDFE and
MMSE–BDFE

6.5.2   Joint Parameter Estimation and Data Detection

The uplink of a CDMA system is considered where K users simultaneously transmit
data packets over K multipath time-invariant channels using binary phase-shift keying
direct sequence spread spectrum (BPSK/DSSS) modulation. The baseband complex
impulse response of the k–th user channel is assumed to consist of L paths, each of
which is characterised by a complex coefficient $g_{k,l}$ and a delay $\tau_{k,l}$. These channel
parameters together with the transmitted energies of all users are arranged in a pa-
rameter vector Θ which is assumed to be unknown at the receiver. The transmitted
symbols of all users in a certain data packet are represented by the matrix $\underline{B}$. With the
above definitions, the received signal $y(t)$ can be written as $y(t) = S(t; \underline{B}, \Theta) + n(t)$,

where $\mathcal{S}(t; \mathbf{E}, \Theta)$ is the superposition of $K \cdot L$ signals contributed by the incident waves and corrupted by zero–mean additive white complex Gaussian channel noise $n(t)$ with $E[n(t+t_0)\, n^*(t)] = N_0\, \delta(t_0)$. An algorithm has been proposed which *jointly estimates the channel parameters and the data bits of all users* [70]. Maximum likelihood (ML) solutions of the problem are given by values $(\mathbf{E}, \Theta)$ which maximise the log-likelihood function $\Lambda(\mathbf{E}, \Theta; y(t)) = 2\int_0^T \mathrm{Re}\{y(t)\mathcal{S}^*(t; \mathbf{E}, \Theta)\}\, dt - \int_0^T |\mathcal{S}(t; \mathbf{E}, \Theta)|^2\, dt$. Since the maximisation of $\Lambda(\mathbf{E}, \Theta; y(t))$ is computationally too intensive, we rely on iterative algorithms to separate the task into several separate optimisation problems. The expectation maximisation (EM) algorithm is used to estimate Θ while the data symbols are detected by means of a multistage detection (MS) algorithm. Both algorithms are combined within a Gauss-Seidel scheme. Monte-Carlo simulations have been carried out, where the symbol energies $\mathbf{E}_k$ of all users at the receiver remain constant during different simulation runs, although the delays and amplitudes vary in a random manner. Fig. 6.33 depicts the uncoded bit error probability $P_{b,1}$ of the first user in a system with $K = 6$ and $L = 3$. In comparison to the RAKE receiver with perfect estimates of the channel parameters, the proposed iterative scheme achieves a substantial improvement in performance. The resulting bit error probability is very close to that of a single-user detector, as denoted by the dotted line (BPSK). Fig. 6.34 shows the bit error probability $P_{b,1}$ for a constant $\gamma_1 = 8$ dB as a function of symbol energies $\mathbf{E}_k$, $k = 2\ldots6$, of the interfering users relative to $\mathbf{E}_1$. Additional simulation results [70] of a two-user system with a data rate of 128 kbit/s using macrocellular channel measurements at carrier frequency 1980 MHz show the capability of the proposed scheme to eliminate the near–far effect even in realistic environments.
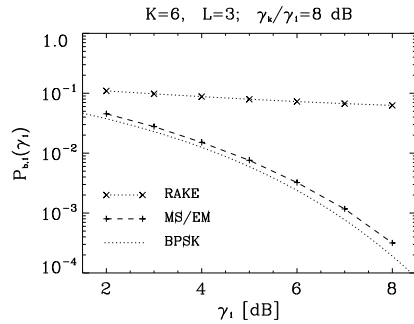

Figure 6.33: Bit error probability $P_{b,1}(\gamma_1)$ of user 1 as a function of the signal–to–noise ratio $\gamma_1 = \mathbf{E}_1/N_0$ in the presence of 5 interfering users with $\gamma_k = \mathbf{E}_k/N_0$, $k = 2\ldots6$
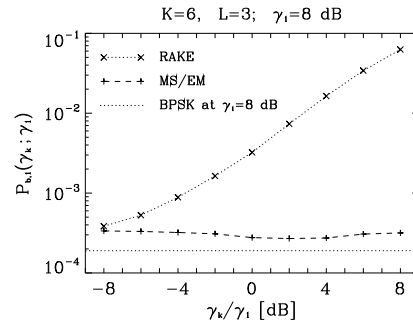
Figure 6.34: Bit error probability $P_{b,1}(\gamma_1)$ of user 1 for constant $\gamma_1 = 8$ dB and various interference levels $\gamma_k = \mathbf{E}_k/N_0$, $k = 2\ldots6$

6.5.3   CDMA with Interference Cancellation

Performance in terms of BER for the uplink of a DS–CDMA communications system using the Interference Cancellation (IC) technique [71, 72] and non coherent reception has been presented in Ricean fading environments. These investigations have been carried out by L. Levi and G. Romano from CSELT, Torino, Italy. The considered propagation channel is affected by Ricean fading, characterised by a ratio ρ between the line of sight and the multipath components; the fading phenomena are assumed independent for the different users. For sake of simplicity, synchronous reception was assumed in the simulations, although the technique can be used also in the asynchronous case [71]. The IC technique considered is based on orthogonal modulation (i.e. Walsh–Hadamard encoding) and on the signal demodulation from the strongest to the weakest one according to a power list. User assigned pseudo noise (PN) sequences are used to distinguish the different signals but do not introduce any spreading. In this way the first signal to be demodulated is the one that presents the highest signal to interference ratio (C/I) and thus it is less impaired by interference. The signal is then cancelled and so the overall C/I ratio increases and also the weaker signals can reach the C/I needed for the required performance. Considering that the base station has to demodulate all the received signals and that it knows all the user–assigned PN codes, it starts the demodulation of the strongest signal on the basis of the received signal power list. The base station performs the descrambling of the received signal with the PN code associated with the strongest user and then the Hadamard decoding by applying a Walsh–Hadamard Transform (WHT) to both the inphase and quadrature signal components. The chosen code word, which is the one with largest modulo value after WHT, is cancelled and the resulting signal is subject to inverse WHT and scrambled with the same PN sequence. The procedure is then iterated with the second signal in the power list. The power list can be obtained in an adaptive way at time T_i by analysing the demodulated signals at time T_{i-1}, where T is the time duration of each Hadamard code word. The signal power is related to its maximal co–ordinates after WHT, thus the power list can be obtained by ordering the maximal co–ordinates of all the demodulated signals. The initial conditions can be achieved either by the power control algorithm or by random initialisation.

A scenario in which 10 active users are simulated has been considered. Each user's signal is encoded with a Hadamard block code $H(128, 7)$, scrambled with the user–assigned PN code and then BPSK modulated; the overall processing gain is $P_g = 128/7$ (12.62dB). The transmitted signals, affected by independent Ricean fading, are summed up at the receiver side to obtain the overall received signal. From the simulated results, it was found that the IC technique allows a greater capacity than the of conventional CDMA, even with a relatively low processing gain. Increasing the number of cancelled interferers improves performance but, on the other hand, the receiver is more complex, and a trade off between complexity and performance has to be found. Performance depends on the Ricean factor ρ, which characterises the propagation channel, and, especially for low factors, the curves with all the inter-

ferers cancelled approach the one user case. The best performance is obtained with $\rho = 10$ dB, while with $\rho = 100$ dB the algorithm cannot work at its best for the first signals to be demodulated and cancelled because the received signals present almost the some power and thus it is not possible to find the strongest one. For $\rho = -100$, 0 and 100 dB, simulations with the computed power list give performances which approach that obtained with the ideal list, while for $\rho = 10$ dB (where errors in the demodulation order are not negligible with respect to the effects of fading) there is a loss of about 1.5 dB in the E_b/N_0 ratio at BER $= 10^{-2}$. Simulation results also show that the adopted interference cancellation technique is less sensitive than conventional CDMA to non perfect power control and chip synchronisation.

A special kind of IC technique, suitable for the synchronous downlink of CDMA systems, has been developed by M. Bossert and T. Frey, University of Ulm, Ulm, Germany. A less complex receiver implementation is achieved by exploiting the restriction of synchronism with suitable spreading codes.

The conventional approaches in JD and IC deal with the general case of a mobile radio link. The asynchronous uplink has different channel impulse responses for each user. The downlink is treated as a special case having some simplifications (because of synchronism and a common impulse response) but is nevertheless a computionally expensive task, especially considering that it has to be performed in the mobile with restrictions on size and power consumptions. For the JD/IC algorithm there are no principal restrictions to the spreading sequences used and quasiorthogonal Gold codes are widely used because of their good correlation properties at a sufficient large code set size.

The inherent synchronism of the downlink allows the use of orthogonal spreading codes. An example is the Qualcomm-System which uses spreading sequences based on scrambled Hadamard codes. These sequences deliver an ideal user separation in AWGN channels because the orthogonality avoids inter–user interference (IUI). With increasing time dispersion of the channel the orthogonality diminishes and turns into a quasiorthogonality, which results in the occurrence of IUI.

The IUI is proportional to the interference parameter

$$I_h := \sum_{k \neq 0} |\varphi_{hh}(k)|^2 \tag{6.4}$$

of the time discrete equivalent channel $h(k)$.

The main idea of this IC technique is to restore the lost orthogonality due to the multipath propagation by applying an equaliser working on the input signal (on chip level) before despreading. Due to the fact, that the equaliser has no knowledge of the despreaded data, only a linear type equaliser is applicable. Although the MMSE criterion is used for coefficient calculation, the resulting noise enhancement limits the performance of IC. Applying a time-invariant (no fading) channel with 3 paths of equal power on a fully loaded system (number of users = spreading length) the loss is about 4dB at a bit error rate of 10^{-3} compared to the single user bound (ideal BPSK). In

terms of the interference parameter I_h, which determines the link performance, the 3-path channel used is worse ($I_h = 0.667$) than the COST207 channel models, where $I_h = 0.28$ is derived from the delay power profile of the typical urban channel.

In order to overcome the penalty of noise enhancement this method was combined with interference estimation and subtracting, cf. Fig. 6.35. The input signal is now
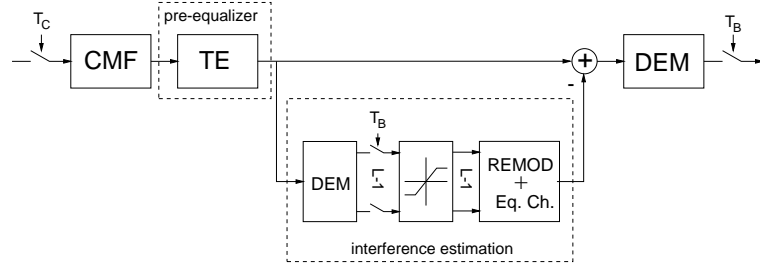

Figure 6.35: Receiver structure

only weakly equalised in order to keep the noise enhancement small. Then the signals of the other users were predemodulated, decided, remodulated and convolved with the equivalent channel, which delivers an estimate for the IUI. In order to keep the effect of error propagation small, the reliability of each decision is considered by a nonlinear characteristic. The estimation of the IUI is subtracted from the input signal. For further details see [73]. This scheme shows that even in the fully loaded case only a slight degradation of approximately 1 dB compared to the optimum single user bound (cf. Fig. 6.36) and thus promises a good performance on mobile radio channels.
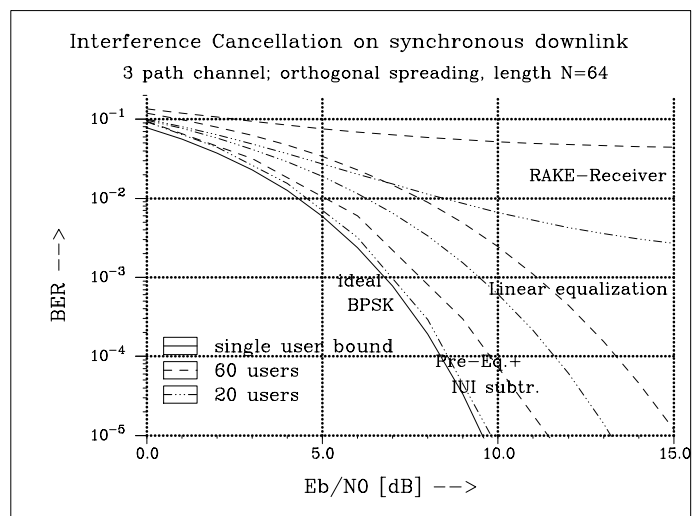
Figure 6.36: Performance comparison of the different receiver types

6.6   Hybrid TDMA/CDMA

A. Burr, University of York, United Kingdom

A number of schemes have been proposed which are hybrids of TDMA and CDMA. The objective of these is to avoid the shortcomings of both TDMA and CDMA, and thus to obtain enhanced capacity. Some of the schemes are also considered in more detail elsewhere in this chapter: the objective here is to show how the inclusion of elements of one scheme may enhance the capacity (or other performance objective) of the other.

6.6.1   TDMA/SFH

The use of slow frequency-hopping has been considered together with coded modulation. The effect of SFH in this context is to enhance the effect of the diversity of the code without requiring long delays due to interleaving. To avoid self–interference, zero–coincidence hopping patterns synchronised among all users would have to be employed in a cellular system. The effect of correlation between the frequency channels is considered, and it is shown that for a separation between hopping frequencies greater than 0.15/(delay spread), the degradation of the system is negligible. It is also shown that performance within 1 dB of ideal is achieved with no more than 5 hopping frequencies.

6.6.2   JD-CDMA

A TDMA element (as well as FDMA) is included in the Joint Detection (JD-CDMA) system developed at the University of Kaiserslautern [74], in a system which is based on DS-CDMA. This system is reviewed in more detail in section 6.5 and in chapter 7. Here we will consider the extent to which the inclusion of FDMA and CDMA elements provide advantages over a pure TDMA or CDMA system.

Firstly, the availability of all three forms of multiple access provides flexibility, since the system is able to switch between them. This is important in a third generation system, since it allows operation in a range of operating environments, for a variety of service types, and supports a range of terminal types. It would also provide interoperability between mobiles and base stations using different types of air interface.

Secondly, it allows the system to take advantage of a wide range of different forms of diversity. Diversity has been identified as essential in overcoming the degrading effects of the mobile radio channel, by reducing the random variation of the signal to interference ratio due to fading, etc. Fig. 6.37 summarises the types of diversity available in any mobile radio system. All these forms are available in the JD–CDMA system because of the availability of CDMA and TDMA. For example, frequency diversity is provided by the CDMA spreading, time diversity by coding and interleaving on a TDMA basis, and interferer diversity through CDMA (which implies that a number of users share the same channel). Various forms of antenna diversity have also been investigated, and offer further improvements.
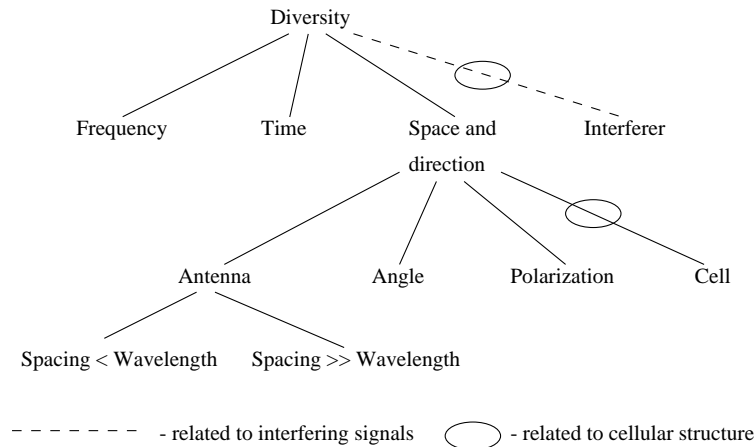
Figure 6.37: Diversity approaches in cellular systems

6.6.3 CTDMA

Coded Time-Division Multiple Access (CTDMA) is also proposed [75]. This is based on TDMA, but the signal is spread in the frequency domain using a pseudo-random code, as in CDMA. The principle is described in chapter 7. Each user's signal is converted to a symbol-by-symbol TDMA waveform. This is convolved with a pseudo–random sequence common to all users within a single cell. At the receiver the signal is passed through the aperiodic inverse filter of the spreading sequence, which in effect reverses the convolution and regenerates the TDMA signal. Hence the users may be perfectly separated. Since the aperiodic inverse filter is not a matched filter the performance is degraded relative to matched filter reception. However, it has been shown that spreading sequences exist for which this degradation is very small, $\approx$ 0.4 dB. These sequences are binary with chip values ± 1, so that the resulting signal is constant envelope.

The above description neglects the effect of multipath, which will cause interference between users occupying adjacent slots. This can be overcome in two ways. For small delay–spreads a guard time may be introduced between users. For delay–spreads significantly greater than the chip period (greater than 5 μs), this would excessively degrade the spectral efficiency. Hence an equaliser must be used in the receiver. It is proposed to use the *Maximum-a-posteriori* (MAP) equaliser, which has optimum performance, and whose complexity is kept within bounds because only a few users will overlap at any one time.

In a cellular system CTDMA would use a different spreading sequence in each of one cluster of cells. In this case inter-cellular interference would appear as uncorrelated noise, as it does in a CDMA system, and therefore 100% frequency re–use is possible

due to the interferer diversity effect. It has been shown that multiple sequences with good interference rejection properties exist.

The advantages of CTDMA over a conventional TDMA system can be summarised as follows:

- The peak–to–mean power ratio of the signal is reduced to unity, giving electro-magnetic compataibility (EMC) advantages

- In a cellular system 100% frequency reuse is possible, as in CDMA systems

- The inherent frequency diversity of DS–CDMA is also available to CTDMA

- Inter–cellular interference reduction techniques such as voice activity detection apply equally to CTDMA as to CDMA

- Since the receiver after the inverse filter is TDMA, the system has a high degree of compatibility with TDMA.

The main disadvantage is the additional complexity of a linear filter of length N in the transmitter, and another of length $3N$ in the receiver.

6.7 Multicarrier techniques

L. Vandendorpe, Universite Catholique de Louvain, Belgium

Multicarrier techniques have been recently considered for transmission over fading channels. These techniques use more than one carrier to transmit the information associated with a particular user. OFDM (Orthogonal frequency division multiplexing) which is a particular case of multicarrier modulation is currently used in the DAB (Digital audio broadcasting) system and is a serious candidate for DVB (Digital video broadcasting) over terrestrial networks. Also OFDM has been seriously investigated for high bit rate transmission over telephone lines. OFDM can be seen as a parallel transmission: the input symbol stream is divided into parallel streams which are used to modulate carriers which are orthogonal on the symbol duration. Hence the symbol duration is increased and the signal should be more resistant to large delay spreads. To state it in the frequency domain the number of carriers should be such that the bandwidth of each of these carriers becomes sufficiently narrow to consider the channel as frequency non–selective. Using this modulation technique the time discrete transmission signal can be calculated in a cost effective way by an IFFT (inverse fast Fourier transform), and an FFT can be used in the receiver. OFDM transmitter and receiver are depicted in Fig. 6.38.

6.7.1 OFDM with guard time

A very elegant way to remove the problem of ISI is to use the technique of guard interval of length T_g. If the channel impulse response is about T_g the OFDM symbols of length T_u can be periodically extended to build a symbol of length $T_g + T_u$. After transmission the first T_g seconds of each OFDM symbol will be corrupted because of the channel impulse response. If the detector uses the last T_u seconds of each symbol this part is not corrupted by the previous OFDM symbol and the subcarriers keep their orthogonality. The signal at the qth output of the FFT device and associated with
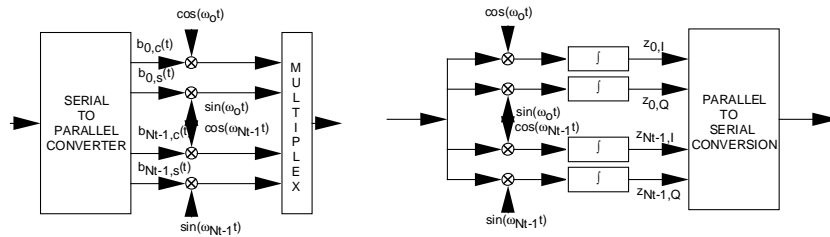

Figure 6.38: OFDM transmitter and receiver

symbol n (I_q^n) is given by

$$y_{g,q}^n = \sqrt{\frac{2P}{N_t}}\, I_q^n\, C(2\pi q/T)\, T + v_{g,q}^n \tag{6.5}$$

where $C(2\pi q/T)$ is the Fourier transformation of the channel impulse response $c(t)$ for frequency $2\pi q/T$ and $v_{g,q}^n$ is the effect of the additive Gaussian noise. Orthogonality between the tones is maintained and ISI is avoided. However the symbol affecting the i-th carrier in the OFDM multiplex is affected by the value of the channel transmittance at that frequency. Assuming that complex gain can be estimated the symbol can be corrected by the receiver. The price to be paid to use guard times is a loss of $T_g/T_g + T_u$ in useful power or an equivalent increase of the bandwidth. How absolute and differential (de)modulations could be performed with OFDM has also been investigated [76]. Differential detection is very attractive, because when the channel can be considered as constant between two successive symbols, its affect is compensated for by the differential detector. Fig. 6.39 shows the sensitivity of OFDM to time variations of the channel. The channel was the Bad Urban defined in COST 207.
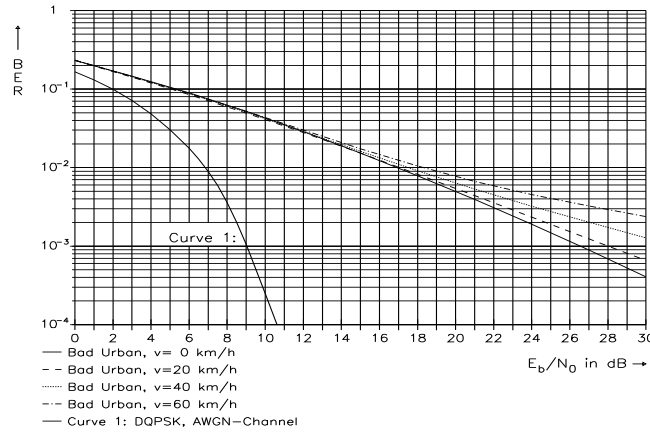

Figure 6.39: Performance of OFDM in the Bad Urban channel for various speeds

OFDM might be used also in an FH (frequency hopping) scenario. In order to avoid a user being allocated to a fading frequency, its frequency is modified according to a specific pattern. The frequencies in the hopping set may be selected such that they are orthogonal and hence this scheme is implemented very easily by means of (I)FFTs. OFDM was also investigated for a radio link at 34 Mbits/s in a bandwidth of 8 MHz. Absolute and differential modulation schemes were compared for AWGN and multipath propagation [77]. A drawback of OFDM signals is the non constant envelope which has a large dynamic. Therefore a power loss has to be accepted in the presence

of a nonlinear device such as a high power amplifier. These aspects were analytically investigated as well.

6.7.2 OFDM without guard time

If OFDM without guard time is used, the system is affected by ISI. Moreover the orthogonality between tones is lost and hence cross–carrier interference (CCI) appears. The efficiency of OFDM transmission over a specular multipath fading channel has been analytically computed in [78]. For a given delay range and assuming Rician distributions of the path gains, it is shown that when the number of tones goes up the system performance improves. However the limiting effect is this scenario would be the channel variations. It is expected that an optimum number of tones could be found. Also it was assumed that the filters in the receiver were matched to the symbol shape only.

6.7.3 OFDM-CDMA

In order to provide the system with a multiple access capability CDMA can be mixed with OFDM. There are two ways to combine OFDM with CDMA.

Method 1

A first possible combination was investigated in [79] for a multiple access and multipath scenario. The transmitted signal is first OFDM modulated and then spreading is put on top of it. Basically this scheme resembles a CDMA system; the main difference is that the spread signal is a multitone signal. This combination benefits from the properties of CDMA as well as from its drawbacks. In [78], the total interference was modelled as Gaussian distributed. To keep the bandwidth constant the chip duration has to be constant and hence longer pseudo–noise codes can be used with larger numbers of tones. Consequently more users can be accommodated in the same bandwidth. Diversity reception was investigated and the computational results show the advantage associated with larger numbers of tones in combatting both the multipath effect and the multiple access interference. For this type of combination the technique of guard interval is no longer relevant. Hence Multiple Input–Multiple Output (MIMO) equalisation structures were investigated for OFDM–CDMA in [80, 81, 82]. The equalisation structures were derived for filters matched to both the channel and the symbol shape. The steady–state behaviour of linear [81] and decision feedback [82] equalisers was investigated. Adaptive versions [80] have also been proposed. Adaptive RLS (recursive least square) structures were derived and presented in the form of a Kalman algorithm. Simulation results obtained for a time–varying channel modeled by means of a tapped delay line show the effectiveness of the equalisation.

For such a system, Joint Detection (JD) was investigated as well. The device processes the outputs of filters matched to the channel and the symbol shape. It turns out that the matched filter outputs suffer from ISI (inter Symbol Interference), IBI
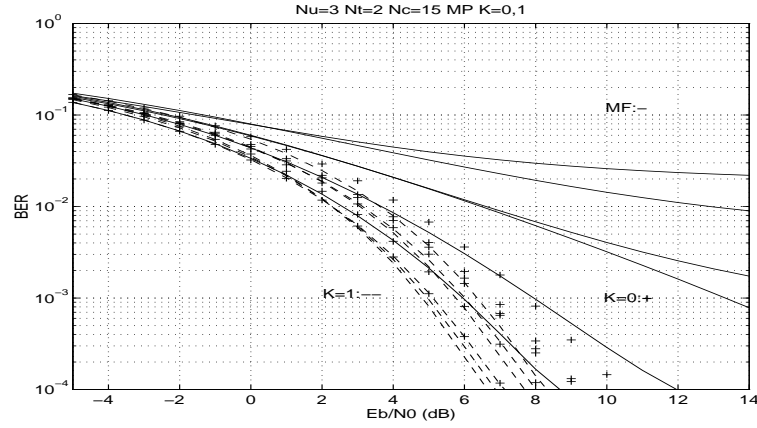
Figure 6.40: BER for $N_c/N_t = 15/2$, $N_u = 3$ users, and channels with 2 paths (equal amplitudes) per user and matched filtering only (MF), interference cancellation only (1 tap filters, $K = 0$), and JEIC with (3 taps filters, $K = 1$).

(Inter Band Interference) and MAI (Multiple Access Interference). The maximum–likelihood sequence estimator was derived for such a system, but is very complex. Therefore suboptimum detectors based on the processing of matched filter outputs were investigated. The receiver contains $N_u \times N_t$ matched filters where N_u and N_t are the number of users and tones respectively. It was first assumed that the channel information was available and hence channel matched–filtering was performed. Then a solution was proposed to perform symbol shape matched filtering only.

When designing joint detection devices the main challenge is to obtain structures whose complexity is only linear with the number of users and which are near–far resistant. That makes it possible to avoid a fine power–control strategy. Different types of joint detection devices were investigated for multipath channels. They do not assume block transmission. These structures are

1. The linear joint detector [83] (T–JEIC, meaning transversal joint equaliser and interference canceller), see Fig. 6.40. The MMSE MIMO joint detector uses coefficients such that the expectation of the error between the true symbols and their prediction built from the sampled matched filter outputs is minimum.

2. The decision feedback detector [84] (DF–JEIC), see Fig. 6.41. Actually two types of DF joint devices have been investigated. In the first one (DF–JEIC–1), the estimates are built from current matched filter outputs, a few future ones and previous decisions. For mathematical tractability it was assumed that the decisions are always correct. In the second device (DF–JEIC–2), the users are
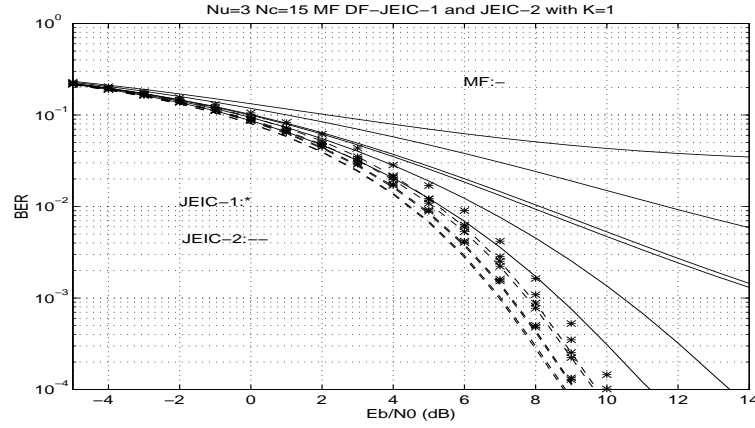
Figure 6.41: Bit error rate as a function of E_b/N_0 for $N_c/N_t = 15/2$ and $N_u = 3$ over one–path asynchronous channels. The solid curves are for matched filtering only (MF), the stars are for DF–JEIC–1 with 3 tap filters and the dotted curves are for DF–JEIC–2 with 3 tap filters.

   ordered in decreasing order of power. The most powerful user is detected with
   the first DF strategy. Then, for the second most powerful user, the estimates are
   built similarly except for the current decision of the strongest user which is used
   instead of the matched filter output, and so on for the other users.

3. The fractionally spaced linear joint detector (FSJD). When the channel is time
   varying, both the channel matched filter and the joint detector have to be adap-
   tive. Rather than performing channel matched filtering, symbol shape matched
   filtering can be performed but in order to be able to render the effect of the chan-
   nel in the adaptive device the sampling rate at the output of the matched filters
   has to be increased. The receiver is then only supposed to know the pseudo–
   noise codes of the users.

All these detectors have been designed for an MMSE criterion. A zero–forcing design
would correspond the an MMSE design at infinite E_b/N_0 ratio. For all these structures,
it has been shown how to obtain the coefficients of the equalisers in close form and
how to adapt them by LMS or RLS techniques. Moreover, from the decision variables
obtained after joint detection, assuming BPSK modulation it has been shown how to
obtain a close form expression of the BER.
The steady–state performance of all these joint detectors has been investigated in asyn-
chronous scenarios with one–path or two–paths per user. Also the resistance against
a near–far effect for the same channels has been demonstrated, see Fig. 6.42. The re-
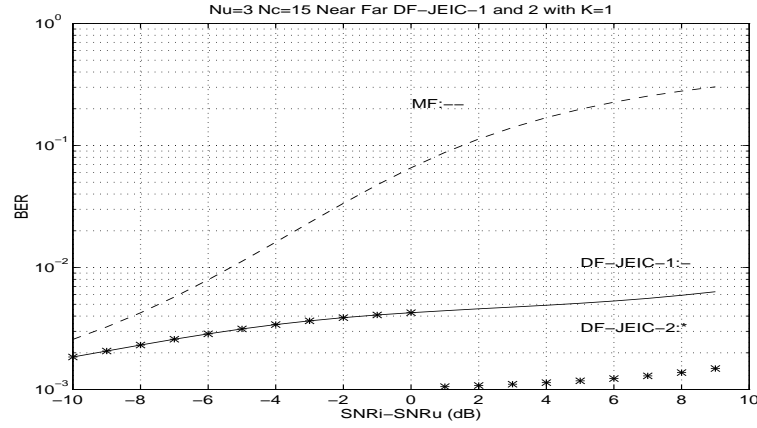
Figure 6.42: Illustration of the near–far resistance for $N_c/N_t = 15/2$ and $N_u = 3$ over one–paths asynchronous channels. $E_b/N_0 = 7$ dB. Matched filter detection (MF), DF–JEIC–1 (solid line) and DF–JEIC–2 (stars) both with 3 taps ($K = 1$).

sults are that, assuming channel matched filtering, and for a constant complexity, DF–JEIC–2 is best, then comes DF–JEIC–1 and then T–JEIC. Decision feedback fractionally spaced joint detection has not yet been studied, but is certainly the most promising candidate.

Method 2

A second method to combine OFDM with CDMA was analysed in [85] for the downlink. Here, spreading is performed on the information symbol level prior to multitone modulation. If N_t subcarriers are available every information symbol of a single OFDM symbol is spread over one subset of M_t subcarriers using M_t–dimensional orthogonal codes. Originally this technique was regarded as a multiple access technique but it can also be regarded as a diversity technique. To obtain a maximum diversity gain, N_t/M_t $(M_t < N_t)$ code sets were used in every OFDM symbol which were arranged like a comb thus minimising the correlation among the subcarriers allocated by a single code set. Since the orthogonality of the codes is destroyed by the channel equalisation is necessary in the receiver. Three different equalisation algorithms were investigated in [85]: Restoring the orthogonality by multiplying the received signal vector with the inverse channel transfer function (ORC) shows poor behaviour in Rayleigh–Fading channels because weak subcarriers cause a high noise amplification. Better results were obtained if only those subcarriers are restored whose power lies above a certain threshold (TORC). The best performance was achieved by an iterative procedure evaluating the Likelihood function of all symbol sequences of code length

M_t with only one bit difference to a starting symbol sequence which was obtained by TORC. The most probable sequence was then used as the starting sequence for the next iteration step. Four iteration steps were sufficient to get an E_b/N_0 gain of more than 8dB at a BER of 10^{-3} in comparsion to a conventional OFDM system (see Fig. 6.43).
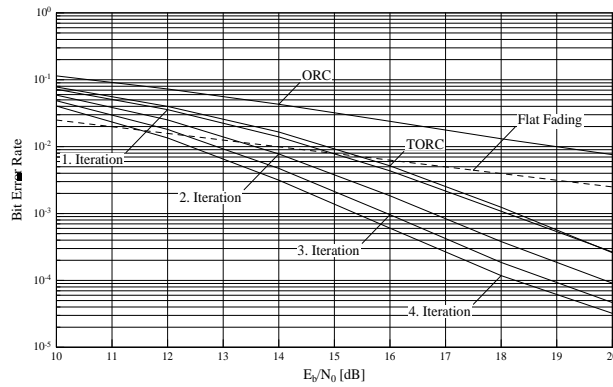
Figure 6.43: BER as function of the average E_b/N_0 for different OFDM–CDMA equalisation algorithms under Rayleigh–Fading conditions. (4–QAM, uncorrelated fading, noisy channel state information $\sigma^2 = 0.1N$, $M_t = 32$)

The idea of OFDM–CDMA has also been investigated in [86] for a DECT–like system. Here, spreading was performed on bit level using orthogonal Walsh codes. With Walsh codes of length four a differential detection structure can be maintained and no channel estimation has to be performed at the receiver.

6.8   MAC Protocols

C.J. Burkley, University of Limerick, Ireland

The Medium Access Control (MAC) sub layer is located between the Data Link Control (DLC) layer and the Physical layer in the OSI Model. Functionally it is a sub layer of the DLC layer and its purpose is to allocate the multi–access medium among several nodes.

A radio medium is generally a broadcast transmission medium unless a special effort is made to focus the transmission in one direction. The radio interface is therefore analogous to a broadcast system rather than to a dedicated line for an individual connection. Thus, a mechanism is required to ensure that users gain access to the medium in a fair manner and also that efficient use is made of the medium.

The two main categories of random access are ALOHA and carrier sense multiple access (CSMA). In CSMA, which is one of the most common accessing techniques in use today, a node wishing to transmit a packet, first listens to the channel to determine whether another user is currently accessing the channel. CSMA is less prone to instability problems than ALOHA and its efficiency can be further improved by using collision detection (CD) so that colliding sources cease to transmit when a collision has been detected rather than waiting until the end of a packet. However CSMA/CD is difficult to implement in a radio environment as it may be difficult for sources to detect a collision in the presence of severe fading. CSMA/CD is also unsuitable for voice traffic because of its unbounded packet delay. Other possible multiple–access techniques are the token ring and token bus, but these schemes are more difficult to manage in the fading radio environment.

There is therefore, a need for a multiple access protocol, which would perform efficiently in the hostile radio environment and which would be suitable for integrating both voice and data traffic.

Packet access mechanisms for cellular radio were consider in the RACE Mobile Telecommunications Project 1043 [87]. The primary advantage of packet transmission is that bandwidth may be allocated on a demand basis. Four different techniques were examined, TM–BCMA/CD (time–multiplexed base–controlled multiple access with collision detection), PRMA (packet reservation multiplex access), HPS–DB (hybrid packet system with dynamic boundary) and HPS–FB (hybrid packet system with fixed boundary) and it was concluded that the PRMA protocol is an attractive candidate for mixed services over a range of cell sizes as it can accommodate fixed channel access, reserved channel access and random channel access.

In the PRMA protocol [88], the channel is divided into slots, which are grouped in frames. Within a frame each slot is recognised as available or reserved on the basis of a feedback packet broadcast in the previous frame from the base station to all the terminals. As in slotted ALOHA, terminals with new information contend for access to available slots. At the end of each slot the base station broadcasts a packet that reports the results of the transmission. A terminal that succeeds in sending a packet to the base station obtains an implicit reservation for exclusive use of the corresponding

time slot in subsequent frames. PRMA requires all terminals to listen to acknowledgements in all slots. Frame reservation multiple access (FRMA) [89], is a variant of this scheme in which the base station broadcasts the acknowledgement for all the slots in a frame at the end of the frame. This results in reduced receiver activity and the system can be further enhanced by using an adaptive permission probability scheme, where the permission probability is chosen depending on the number of reserved slots at the beginning of the frame.

In order to support synchronous and isochronous services, while guaranteeing acceptable grade–of–service some kind of isochronous circuit allocation capability has to be provided by the MAC sublayer and a Space Division Multiple Access (SDMA) protocol with reservation demand assignments (DA) discipline to provide hybrid packet and circuit switching services has been proposed [90]. The channel timing format is a slotted channel, each time slot corresponding to the packet size of the lower bit rate service provided by the network. Packets corresponding to different services are integer multiples of slots. Slots are grouped onto fixed frames and the number of slots in a frame is calculated so that the delay between two consecutive voice packets does not affect the quality of speech. Slots are divided into reservation slots and data transmission slots and the number of slots for each class can be modified as a function of the collision rate or the number of re transmissions.

Polling can also be used as a technique for controlling access to the medium and a number of different multiple access techniques including full polling, partial polling and a contention protocol within a polling structure have been proposed and investigated [91] for their suitability for an integrated voice/data indoor radio system. Results showed that 2.5 Mbits/s user data throughput can be supported with the partial polling or contention schemes with a 20 ms frame length and with acceptable voice delays.

A new transmission/resource sharing scheme which uses a pure RTS (Request to Send)/CTS (Clear to Send) protocol has been proposed [92] as a resource sharing scheme for radio LANs. In this scheme the available bandwidth is divided into sub–bands and when a base station has a message to send it sends an RTS over an primary sub–band that was not busy to the destination station which was also not busy. The source station then listens to that set of sub–bands for a CTS from the destination. If the RTS is received intact at the destination a CTS is sent to the source over the set of sub–bands. On receiving the CTS, the source station sends the data over the set of sub–bands. On receiving the data the destination sends an acknowledgement back over the sub–bands.

Since the deployment of new personal telecommunications networks is likely to occur simultaneously with that of new broad band networks the MAC protocol data unit structure should be compatible with the ATM cell structure, which is based on a fixed packet size including a virtual circuit identifier. The need for an additional header (for synchronisation addressing) in the air interface has been identified [90] as well as the need to handle error control for the radio channel. ATM will offer a flexible transfer capability to all services supported by the radio network.

An important feature of the system, related to its spectrum efficiency and its quality

of service, is the channel assignment policy. For non–uniform traffic conditions, dynamic channel allocation (DCA) schemes, in which channels are assigned on demand, out performed fixed channel allocation (FCA) schemes. Hybrid channel allocation (HCA) schemes, in which only some of the available channels are assigned permanently and the remainder are shared dynamically may be simpler to implement and their performance would be somewhere in–between DCA and FCA.

A MAC protocol for ATM–based Indoor Radio Networks has been proposed [93] which uses a request/permit mechanism to control the access to the shared medium. Each remote station declares its required capacity by sending requests to the access control located in the base station. The available capacity is allocated by means of a strategy which approximates a global FIFO queue in such a way that the peak bit rate is enforced and fair access is achieved. The remote stations are informed about the obtained capacity by means of permits, which authorise the remote station to send a cell. The MAC protocol is thus cell based, meaning that an issued permit initiates the transmission in a single cell.

To meet the requirements of future systems in the fading mobile environment an efficient channel management system is needed. The system should include a flexible multiple access technique and dynamic channel assignment. To be compatible with future B–ISDN, the application of ATM is an obvious choice. However, even though some media access systems have been suggested further work needs to be done before a universal system can be proposed.

6.9 References

[1] ITU-T: Transmission Planning Aspects of the Speech Service in Digital Public Land Mobile Networks. Recomendation G.173, March 1993

[2] A.A.M. Saleh, R.A. Valenzuela: A statistical model for indoor multipath propagation. IEEE SAC, February 1987

[3] J.G. Proakis: Digital Communications, Second Edition. McGrawHill Inc, New York, 1983

[4] J.P.M.G. Linnartz, A.J.'t Jong: Average bit error rate for coherent detection in micro and macro cellula. Proc. 6th IEE Int. Conf. on Mobile Radio and Personal Communications, Warwick, UK, 9-12 December 1991

[5] J.B. Anderson: Propagation parameters and bit errors for a fading channel. COMMSPHERE 91, Herzlia, Israel, December 1991, paper 8.2

[6] F.J. Casadevall, A. Valdovinos: Performance analysis of M–QAM modulations applied to the LINC transmitter. IEEE Trans. on Vehicular Technology, Vol. 42, No. 4, November 1993, pp. 399-406

[7] S.A. Hetzel, A. Bateman, J.P. McGeehan: A LINK transmitter. Proceedings 41st, IEEE Vehicular Technolmogy Society Conference, St Louis, USA, pp. 133-137

[8] G. Kaleh: Simple coherent receiver for partial response continuous phase modulation. IEEE JSAC, Vol. 7, No. 9, December 1989, pp. 1427-1436

[9] F. de Jager, C. B. Dekker: Tamed frequency modulation, a novel method to achieve spectrum economy in digital transmission. IEEE Trans. on Commun., Vol. COM-26, May 1978, pp. 534-542

[10] M. V. Eyuboglu, S. Qureshi: Reduced-state sequence estimation with set partioning and decision feedback. IEEE Trans. on Commun., Vol. COM-36, January 1988, pp. 13-20

[11] F. Morales - Moreno, W. Holubowicz, S. Pasupathy: Optimization of trellis coded TFM via matched codes. IEEE Trans. on Commun., Vol. COM-42, February-April 1994, pp. 1586-1594

[12] L. B. Lopes: Relationship between performance and timing recovery mechanisms for a DECT link in dispersive channels. Elect. Letters, 1993, pp. 2173-2174

[13] I. Crohn: Short term modelling of the land mobile radio channel. Doct. Thesis, TU Wien, 1991

[14] D. Saha, T. G. Bridsall: Quadrature - quadrature phase-shift keying. IEEE Trans. on Commun., Vol. COM-37, No. 5, May 1989, pp. 437-448

[15] T. Javornik, G. Kandus: QMSK modulation technique in mobile radio channel environment. IEEE 2nd Symposium on Commun. and Vehicular Tech. in the Benelux, Louvain-la-Neuve, Belgium, November 1994, pp.20-27

[16] J. B. Andersson, T. Aulin, C. Sundberg: Digital phase modulation. Plenum Press, New York, 1986

[17] A. Rodrigues, A. Albuquerque: Digital signatures of M-QAM and CPM systems in a static two–path channel. Internal report, Inst. Superior Técnico, Lisbon, Portugal, January 95

[18] COST 207 - Digital land mobile radio communications. Final report, CEC, 1989

[19] U. Dersch, J. Delgado: CODIT model for propagation. RACE Mobile Telecommun. Workshop, Metz, France, June 1993, pp. 373-377

[20] A. Rodrigues, L. Vandendorpe, A. Albuquerque: Performance of direct–sequence spread spectrum multi–h CPM in indoor mobile radio systems. 44th IEEE Vehicular Tech. Conf. (VTC'94), Stockholm, Sweden, June 1994, pp. 578-581

[21] A. Rodrigues, L. Vandendorpe, A. Albuquerque: Diversity techniques in indoor mobile radio with DS–CDMA multi–h CPM. IEEE 5th Int. Symposium on Personal, Indoor and Mobile Radio Communications (PIMRC'94), The Hague, The Netherlands, Sept. 1994, pp. 1383-1387

[22] R. Podemski, W. Holubowicz: Influence of average number of the nearest neighbours on the optimum choice of CPM signals. RR-30/1993, Franco–Polish School of New Information and Communication Technologies, Poznan, Poland, August 1993

[23] I. Crohn, G. Schultes, R. Gahleitner, and E. Bonek: Irreducible error performance of a digital portable communication system in a controlled time–dispersion indoor channel. IEEE J. Select. Areas Comm. vol. SAC–11, 1993, pp. 1024–1033

[24] I. Crohn., G. Schultes, R. Gahleitner, and E. Bonek: Error floor mechanisms in indoor digital portable communications. Proc. 3rd IEEE Internat. Symp. on Personal, Indoor and Mobile Radio Comm., Boston (MA), Okt 1992, pp. 320–328.

[25] J. B. Andersen, S. L. Lauritzen, and C. Thommesen: Distribution of phase derivatives in mobile communications, Proc. IEE Part H, vol. 137, 1990, pp. 197–204

[26] G. Schultes and J. Fuhl: Phasor explanation of error mechanisms for MSK Transmission over a slightly dispersive radio channel. Proc. Melecon 94, Antalya, 38–42 (1994).

[27] A.F. Molisch, J. Fuhl, and P. Proksch: Error floor of MSK modulation in a mobile–radio channel with two independently–fading paths. IEEE Trans. Vehicular Techn., in press.

[28] V. Lipovac and A.F. Molisch: On the performance of MSK signal transmission over a multipath channel with small time dispersion. IEEE Vehicular Technology Conf. 1995, Chicago 1995, 1995, pp. 25–29

[29] A.F. Molisch and J. Fuhl: Bit error probability of differentially detected (G)MSK in indoor mobile radio channels. 46th IEEE Vehicular Techn. Conf., Atlanta 96, in press (1996).

[30] I. Crohn, and E. Bonek: Modeling of intersymbol–interference in a Rayleigh fast–fading channel with typical delay power profiles. IEEE Trans. on Vehicular Technology 41, 1992, pp. 438–447.

[31] G. Ungerboeck: Channel coding with multi-level/phase signals. IEEE Trans. inform. Theory, Vol. 28, January 1982, pp. 55-67

[32] H. Imai, S. Hirakawa: A New multilevel coding technique using error correcting codes. IEEE Trans. Inform. Theory, Vol. IT-23, No. 3, May 1977, pp371-377

[33] N. Seshadri, C.E.W Sundberg: Multilevel coded modulation for fading channels. Proc. 5th Int. Tirrenia workshop, Elsevier, 1992, pp. 305-316

[34] A.G. Burr: Optimised multistage coded modulation design for Rayleigh fading channels. IEEE Int. Symp. on Information Theory, Vancouver, Canada, September 1995

[35] K. Boulle-Leeuwin, J.C. Belfiore, G. Kawas-Kaleh: Chernoff bound of trellis coded modulation over correlated fadings channels. IEEE Trans. on Comm., Vol. 42, No. 8, August 1994, pp. 2506-2512

[36] K. Boulle, G. Femenias, R. Agusti: An overview of trellis coded modulation research in COST231. PIMRC'94 conference, pp. 105-109

[37] C. Mourot: A high bit rate transmission technique in mobile radio cellular environment. IEEE VTC conference, Denver, May 1992, pp. 740-743

[38] A. Wautier, C. Mourot, J.L. Dany: Phase correcting filters for sub–optimum equalizers. International Zurich Symposium on Digital Communication, 1994

[39] K. Wesolowski, R. Krenz, K. Das: Efficient receiver structure for GSM mobile radio. International Journal of Wireless Information Networks, Plenum Press, 1995

[40] M. Reinhardt, J. Lindner: Vector Decision Feedback Equalization for M–ary orthoginal transmission over multipath channels. 3rd International Symposium on communication theory and applications, Charlotte Mason College, Ambleside, Lake District, UK, July 1995, pp. 166-173

[41] G. Ungerboeck: Adaptive maximum likelihood receiver for carrier modulated data transmission systems. IEEE Trans. on Comm., Vol. 32, 1984, pp. 624-636

[42] R. Krenz, K. Wesolowski: Comparison of several space diversity techniques for MLSE receivers in mobile communications. Proc. Personal, Indoor and Mobile Communications (PIMRC 94), den Haag, September 94

[43] A. Valdovinos, F.J. Casadevall: Equalization and space diversity techniques in mobile environments. IEEE Network, Vol. 8, No. 2, March-April 1994, pp. 36-42

[44] M.L. Moher, J.H. Lodge: TCMP - a modulation and coding strategy for Rician fading channels. IEEE Journal of selected Areas in Communications, Vol. 7, No. 9, December 1989

[45] A.G. Burr: Bounds and estimates of the uplink capacity of cellular systems. Proc. IEEE 44th Vehicle Technology Conference, Stockholm, VTC'94, pp. 1480-1484

[46] A.G. Burr, T.C. Tozer, S.J. Baines: Capacity of an adaptive TDMA cellular system: comparison with conventional access schemes. IEEE Conference on Personal, Indoor and Mobile Radio Communications, PIMRC'94, The Hague, Netherlands, 1994

[47] M. Streeton, A. Urie: System model for adaptive cellular mobile systems. Proceedings of International Conference on Universal Personal Communications, ICUPC'93, 1993

[48] C. van den Broeck, D. Sparreboom, R. Prasad: Performance evaluation of Packet Reservation Multiple Access protocol using steady–state analysis of a Markov chain model. Proc. Joint COST 231/227 Workshop, Limerick, Ireland, pp. 454-462 (Publ. University of Limerick)

[49] M. Mastroforti: Uplink capacity evaluation of a PRMA based system in a terrestrial radio mobile environment. Proc. Joint COST 231/227 Workshop, Firenze, Italy, 1993 (Publ. Kluwer)

[50] J.M. de Vile: A reservation-based multiple access scheme for future universal mobile telecommunications system. Proc. European Conference on Mobile and personal Communications, 1993 (Publ. IEE, U.K.)

[51] A. Klein, P. W. Baier: On the capacity of discrete–time synchronous Gaussian CDMA and TDMA channels. International Journal of Electronics and Communications, Vol. 48, January 1994, pp. 28-33

[52] A.G. Burr: Bounds on spectral efficiency of coded CDMA and FDMA/TDMA. Colloquium on spread spectrum techniques for radio communication systems, London, 27th April 1993 (Publ. IEE)

[53] H. Hashemi: Simulation of the urban radio propagation channel. IEEE Trans. Veh. Technology, Vol. VT-28, August 1979, pp. 213-224

[54] K.S. Gilhousen, I.M. Jacobs, R. Padovani, A. Viterbi, L.A. Weaver Jr, C.E. Wheatley III: On the capacity of a cellular CDMA system. IEEE Trans. Veh. Technology, Vol. VT-40, May 1991, pp. 303-312

[55] J.J.Olmos, R.Agustí: Performance Analysis of a Second Order Delay-Lock Loop with Application to a CDMA System with Multipath Propagation. In 1st International Conference on Universal Personal Communications (ICUPC'92), Dallas (Texas), September 1992

[56] R. A. Iltis: Joint Estimation of PN Code Delay and Multipath Using the Extended Kalman Filter. IEEE Trans. on Comm., Vol. 38, No. 10, October 1990

[57] P. Díaz, R. Agustí: A PN Code Delay Estimator Based on the Extended Kalman Filter for a DS/CDMA Cellular System. Proceedings of the 4th International Symposium on PIMRC, September 1993

[58] C.A.F.J. Wijffels, H.S. Misser, R. Prasad: A Micro–cellular CDMA System over Slow and Fast Rician Fading Radio Channels with Forward Error Correction Coding and Diversity. IEEE Transactions Vehicular Technology, Vol. 42, November 1993, pp. 570-580

[59] G.J.M. Janssen, R. Prasad: Propagation measurements in an indoor radio environment at 2.4 GHz, 4.75 GHz and 11.5 GHz. Vehicular Technology Society 42nd VTS conference frontiers of Technology, Denver, Colorado, 10-13 May 1992, pp. 617-620

[60] L.Vandendorpe, R.Prasad, R.G.A. Rooimans: Hybrid Slow Frequency Hopping/Direct Sequence Spread Spectrum Communications systems with B– and Q–PSK Modulation in an Indoor Wireless Environment. Proceedings of the Fourth International Symposium on Personal, Indoor and Mobile Radio Communications, Yokohama, Japan, September 9-11 1993, pp. 498-502

[61] A. Klein, P.W. Baier: Simultaneous cancellation of cross interference and ISI in CDMA mobile radio communications. Proc. IEEE International Symposium on Personal, Indoor and Mobile Radio Communications (PIMRC '92), Boston, USA, 1992, pp. 118-122

[62] A. Klein, P.W. Baier: Linear unbiased data estimation in mobile radio systems applying CDMA. IEEE Journal on Selected Areas in Communications, Vol. 11, 1993, pp. 1056-1066.

[63] P. Jung, J. Blanz, P.W. Baier: Coherent receiver antenna diversity for CDMA mobile radio systems using joint detection. Proc. IEEE International Symposium on Personal, Indoor and Mobile Radio Communications (PIMRC '93), Yokohama, 1993, pp. 488-492

[64] B. Steiner, P.W. Baier: Low cost channel estimation in the uplink receiver of CDMA mobile radio systems. Frequenz 47, 1993, pp. 292-298

[65] A. Klein, G.K. Kaleh, P.W. Baier: Equalisers for multi–user detection in code division multiple access mobile radio systems. Proc. IEEE International Conference on Vehicular Technology (VTC '94), Stockholm, 1994, pp. 762-766

[66] P. Jung, J. Blanz, M. Naßhan, P.W. Baier: Simulation of the uplink of JD–CDMA mobile radio systems with coherent receiver antenna diversity. Wireless Personal Communications, Vol. 1, 1994, pp. 61-89

[67] M. Naßhan, P. Jung: New results on the application of antenna diversity and Turbo–Codes in a JD–CDMA mobile radio system. Proc. IEEE International Symposium on Personal, Indoor and Mobile Radio Communications (PIMRC '94), The Hague, Netherlands, 1994, pp. 524-528

[68] J. Blanz, A. Klein, M. Naßhan, A. Steil: Performance of a cellular hybrid C/TDMA mobile radio system applying joint detection and coherent receiver antenna diversity. IEEE Journal on Selected Areas in Communications, Vol. 12, 1994, pp. 568-579

[69] M. Naßhan, A. Steil, A. Klein, P. Jung: Downlink cellular radio capacity of a joint detection CDMA mobile radio system. Proc. IEEE International Conference on Vehicular Technology (VTC '95), Chicago, 1995

[70] D. Dahlhaus, A. Radović, B.H. Fleury: Joint Parameter Estimation and Data Detection for DS/SSMA Systems Operating in Time–Dispersive Channels. ITG-Fachtagung "Mobile Kommunikation", Neu-Ulm, Germany, 1995

[71] P. Dent, B. Gudmundson, M. Ewerbring: CDMA–IC: a novel code division multiple access scheme based on interference cancellation. Proc. IEEE International Symposium on Personal, Indoor and Mobile Radio Communications (PIMRC '92), Boston, 1992

[72] L. Levi, F. Muratore, G. Romano: Simulation results for a CDMA interference cancellation technique in a Rayleigh fading channel. International Zurich Seminar on Digital Communications, Zurich, March 1994.

[73] M. Bossert, T. Frey, T: Interference cancellation in the synchronous downlink of CDMA-systems. ITG-Fachtagung "Mobile Kommunikation", Neu-Ulm, Germany, 1995

[74] P. Jung, J. Blanz, M. Nasshan, P.W. Baier: Simulation of the uplink of JD-CDMA mobile radio systems with coherent receiver antenna diversity. Wireless Personal Communications, Vol. 1, 1994, pp 61-89

[75] J. Ruprecht, F.D. Neeser, M. Hufschmid: Code time division multiple access: An indoor cellular system. Proc. of the 42nd IEEE Vehicular Technology Conference, Denver, 1992

[76] C. Reiners, H. Rohling: Multicarrier transmission technique in cellular mobile communications systems. Proc. IEEE Vehicular Technology Conference (VTC'94), Stockholm, 1994, pp. 1645-1649

[77] V. Engels, H. Rohling: Differential modulation techniques for a 34 Mbit/s radio channel using orthogonal frequency division multiplexing. Accepted for publication in Wireless Personal Communications - Special Issue on Multi-Carrier Communications, Kluwer Academic Publishers, to be published 3rd quarter 1995

[78] L. Vandendorpe: Multitone system in an unlimited bandwidth multipath Rician fading environment. Proc. IEE Conference on Mobile and Personal Communications (MPC'93), Brighton, 1993, pp. 114-119

[79] L. Vandendorpe: Multitone Spread Spectrum Communications Systems in a Multipath Rician Fading channel. IEEE Transactions on Vehicular Technology, Vol. 44, No. 2, 1995, pp. 327-337

[80] O. van de Wiel, L. Vandendorpe: Adaptive equalization structures for multitone CDMA systems. Proc. Fifth IEEE International Symposium on Personal, Indoor and Mobile Radio Communications (PIMRC'94), The Hague, Netherlands, 1994, pp. 253-257

[81] L. Vandendorpe, O. van de Wiel: Performance analysis of linear MIMO equalizers for multitone DS/SS systems in multipath channels. Accepted for publication in Wireless Personal Communications - Special Issue on Multi-Carrier Communications, Kluwer Academic Publishers, to be published 3rd quarter 1995

[82] L. Vandendorpe, O. van de Wiel: Performance analysis of MIMO DFE equalisation of multitone SS signals, IEEE Vehicular Technology Conference (VTC'95), Chicago, 1995, pp. 394-398

[83] L. Vandendorpe, O. van de Wiel: Performance analysis of linear joint equalization and interference cancellation for multitone CDMA. Accepted for publication in Wireless Personal Communications, August 1995.

[84] L. Vandendorpe, O. van de Wiel: Decision-feedback joint detection for multitone CDMA. Paper invited for the Seventh Tyrrhenian International Workshop on Digital Communications, Viareggio, 1995.

[85] T. Müller, H. Rohling, R. Grünheid: Comparison of different detection algorithms for OFDM-CDMA in broadband Rayleigh fading, IEEE Vehicular Technology Conference (VTC'95), Chicago, 1995, pp. 835-838

[86] O'Neil, L. B. Lopes: A simple OFDM transmission scheme for small dispersion environments. To appear at the European and Mobile Communications Conference, Bologna, 1995

[87] J. Dunlop: Packet access mechanisms for cellular radio. Electronics and Communication Eng Jnl., Vol. 5, June 1993, pp. 173-179

[88] D.J. Goodman et al.: Packet reservation multiple access for local wireless communications. IEEE Trans, Vol. COM-37, August 1989, pp. 885-890

[89] P. Narasimhan, R. Yates and D.J. Goodman: Performance analysis of frame reservation multiple access. 3rd International Conference on Universal Personal Communications Record, San Diego, September 1994, pp. 26-30

[90] I. Berberana, J. Jimenez, F.J. Gavilan: A packet media access protocol for mobile networks. Ann. Telecommun (France) Vol. 47, pp. 235-42, May-June 1992

[91] C.J. Burkley and M.P. Moroney: Two new hybrid multiple access protocols for indoor wireless communications. Proc. 1992 URSI ISSSE, Paris, France, September 1992, pp. 701-703

[92] S.A. Black, M. Smith, T.A. Wilkinson: Analysis of a wireless LAN MAC protocol. ETSl RES 10R 92/35, November 1992

[93] C. Blondia, O. Casals, J. Garcia: Performance analysis of a MAC protocol for a broad band network access facility. Symp. on Teletraff. Anal. of ATM Systems '93, Eindhoven 1993